2018

Molecular Level Encapsulation of Chromophores Using Pillar[5]arenes for Enhanced Photostability

Manik Gudimani
South Dakota State University

MOLECULAR LEVEL ENCAPSULATION OF CHROMOPHORES USING PILLAR[5]ARENES FOR ENHANCED PHOTOSTABILITY

BY

MANIK GUDIMANI

A thesis submitted in partial fulfillment of the requirements for the

Master of Science

Major in Chemistry

South Dakota State University

2018

MOLECULAR LEVEL ENCAPSULATION OF CHROMOPHORES USING PILLAR[5]ARENES FOR ENHANCED PHOTOSTABILITY

Manik Gudimani

This thesis is approved as a creditable and independent investigation by a candidate for the Master of Science in Chemistry degree and is acceptable for meeting the thesis requirements for this degree. Acceptance of this thesis does not imply that the conclusions reached by the candidate are necessarily the conclusions of the major department.

Cheng Zhang, Ph.D.
Thesis Advisor

Douglas Raynie, Ph.D.
Head, Department of Chemistry
and Biochemistry

Dean, Graduate School

ACKNOWLEDGEMENTS

I would like to thank South Dakota State University for providing me the opportunity to pursue my master's degree. Also, I would like to thank Dr. Cheng Zhang for advising me and letting me continue with research work. Under his tutelage, I have learned a substantial amount about organic chemistry and his passion for chemistry has inspired me to be a lifelong learner. Other faculty members, have made me realize my strengths and weaknesses, which in turn has made me realize where I can improve and grow as a chemist. Also, I would like to thank all previous and current group members for their help in lab. Most importantly, I would like to acknowledge the love and support of my wife and family—who have ultimately motivated and financed me in achieving my goal.

TABLE OF CONTENTS

LIST OF STRUCTURES

2,2,6,6-tetramethylpiperidine (TMP)	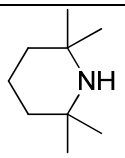
2,2,6,6-tetramethyl-1-phenylpiperidine	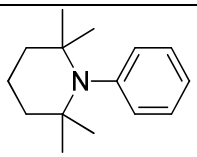
1-(4-bromophenyl)-2,2,6,6-tetramethylpiperidine	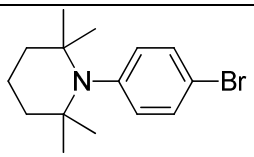
4-(2,2,6,6-tetramethylpiperidin-1-yl)benzaldehyde	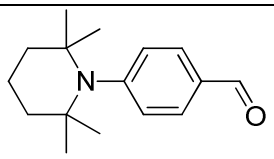
(E)-3-(4-(2,2,6,6-tetramethylpiperidin-1-yl)phenyl)acrylaldehyde **(DB1)**	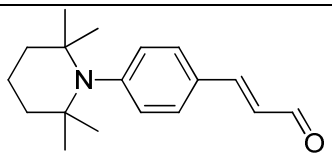
(2E,4E)-5-(4-(2,2,6,6-tetramethylpiperidin-1-yl)phenyl)penta-2,4-dienal **(DB2)**	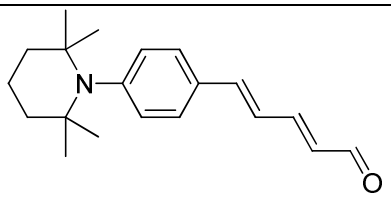
(2E,4E,6E)-7-(4-(2,2,6,6-tetramethylpiperidin-1-yl)phenyl)hepta-2,4,6-trienal **(DB3)**	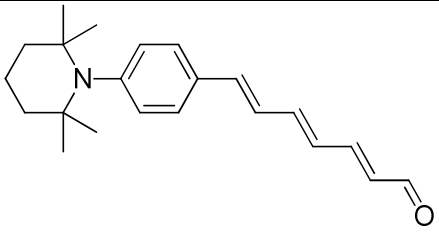
2-methoxyethanol	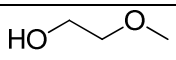

2-methoxyethyl 4-methylbenzenesulfonate	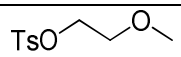
2-(2-(2-methoxyethoxy)ethoxy)ethanol	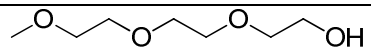
2-(2-(2-methoxyethoxy)ethoxy)ethyl 4-methylbenzenesulfonate	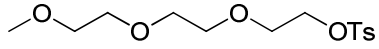
1,4-dimethoxypillar[5]arene	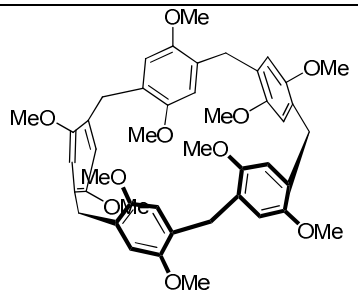
1,4-dihydroxypillar[5]arene	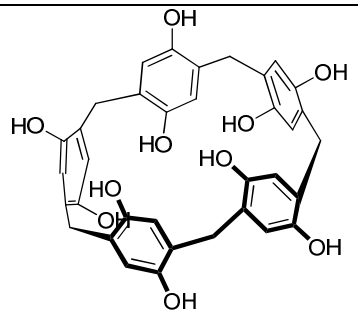
1,4-bis(2-methoxyethoxy)pillar[5]arene	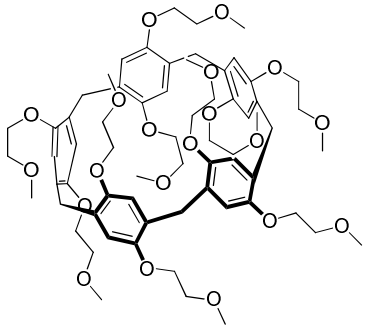

1,4-bis(2-(2-(2-methoxyethoxy)ethoxy)ethoxy)pillar[5]arene	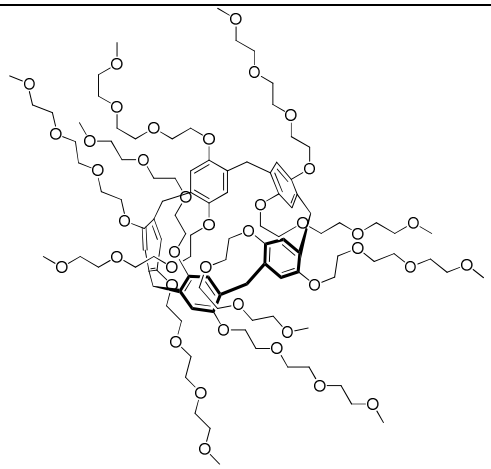
2-(3-cyano-4,5-dimethyl-5-(trifluoromethyl)furan-2(5H)-ylidene)malononitrile **(CF_3-TCF)**	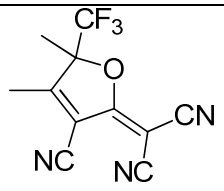
(E)-2-methyl-N-((2E,4E)-6-(trimethylsilyl)hexa-2,4-dien-1-ylidene)propan-2-amine	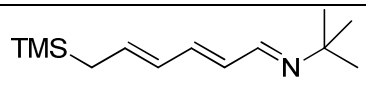
((1,3-dioxolan-2-yl)methyl)triphenylphosphonium bromide	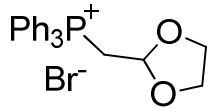
2-(3-cyano-4-((1E,3E)-3-(6-((E)-4-(diethylamino)styryl)-2',6'-dimethoxy-4,4-dimethyl-4,5-dihydro-[1,1'-biphenyl]-2(3H)-ylidene)prop-1-en-1-yl)-5-methyl-5-(trifluoromethyl)furan-2(5H)-ylidene)malononitrile **(CC10)**	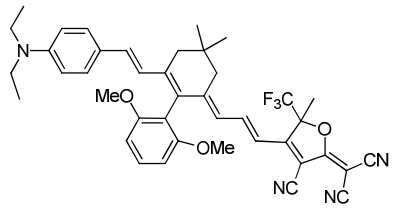

2-(4-((1E,3E)-3-(3-((E)-4-(bis(2-((tert-butyldimethylsilyl)oxy)ethyl)amino)styryl)-5,5-dimethylcyclohex-2-en-1-ylidene)prop-1-en-1-yl)-3-cyano-5,5-dimethylfuran-2(5H)-ylidene)malononitrile (**CLD1)**	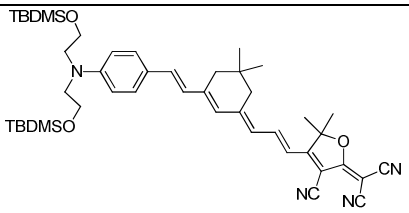

LIST OF SCHEMES

LIST OF FIGURES

ABSTRACT

MOLECULAR LEVEL ENCAPSULATION OF CHROMOPHORES USING PILLAR[N]ARENES FOR ENHANCED PHOTOSTABILITY

MANIK GUDIMANI

2018

Organic π-conjugated materials have been researched extensively for a number of applications including organic photovoltaics, electrooptic (EO) modulation, solid-state lasing, organic light emitting diodes (OLEDs), biological imaging and sensing, chemical sensing and ligands for photocatalysts. These organic optoelectronic materials have one major issue that affects its performance and lifetime—photostability. For some applications, hermetical packaging, which is expensive, is required to prevent degradation by light and oxygen. Photooxidation occurs when a material is exposed to light and causes structural and chemical changes leading to photodegradation of the material. The two primary degradation mechanisms responsible for photooxidation involve superoxide radical anion and singlet oxygen. The state-of-the-art electrooptic chromophores typically contain multiple C=C bonds, which are susceptible to reaction with singlet oxygen, so, protection of C=C bonds via molecular level encapsulation is a promising way to enhance photostability of EO chromophores.

Pillar[n]arenes are a class of cylindrical molecules reported in 2008. A lot of research has been conducted on their synthesis, modification, complexation with host molecules, and formation supramolecular structures. Their sizes, ease of modification and perfect cylindrical shape make them the best structures among known macrocyclic

molecules (e.g., cyclodextrins, calixarenes and cucurbiturils) for encapsulation of chromophores. However, molecular encapsulation using pillar[n]arenes have not been reported. This research aims to develop the first EO chromophore that is encapsulated by a pillar[n]arene and conduct a comparative study of rate of photooxidation to assess the effect of encapsulation on photostability. This research paves the way for future research on photodegradation mechanisms of encapsulated chromophores, and more complete encapsulation of photooxidation-sensitive moieties.

An EO chromophore consists of an electron donor such as an amino group, a pi-conjugation bridge, and an electron acceptor. An encapsulated chromophore is synthesized from coupling of a donor-bridge compound and an acceptor compound in presence of a pillar[5]arene. To make sure the pillar[5]arene in the molecular package does not slip away from the donor end, a bulky amino group, 2,2,6,6-tetramethylpiperidine,TMP, is used as the donor. To ensure the bridge structure can fit into the cavity of the pillar[5]arene, phenylpolyenal bridges of different length were synthesized: (E)-3-(4-(2,2,6,6-tetramethylpiperidin-1-yl)phenyl)acrylaldehyde (DB1), (2E,4E)-5-(4-(2,2,6,6-tetramethylpiperidin-1-yl)phenyl)penta-2,4-dienal (DB2), (2E,4E,6E)-7-(4-(2,2,6,6-tetramethylpiperidin-1-yl)phenyl)hepta-2,4,6-trienal (DB3). DB3 was primarily used due to its optimal chromophore length and ease of encapsulation compared to other donor-bridges. The acceptor 2-(3-cyano-4,5-dimethyl-5-(trifluoromethyl)furan-2(5H)-ylidene)malononitrile (CF_3-TCF) was also selected, which is bulky enough to prevent the pillar[5]arene from slipping away from the acceptor end. Three versions of pillar[5]arenes were also synthesized with different side groups:1,4-dimethoxypillar[5]arene , 1,4-dihydroxypillar[5]arene , 1,4-bis(2-

methoxyethoxy)pillar[5]arene and 1,4-bis(2-(2-(2-methoxyethoxy)ethoxy)ethoxy)pillar[5]arene . Combination of donor-bridge, acceptor and pillar[5]arene produced a series of molecularly encapsulated chromophores (MECs). However, only the MEC (CC14) from DB3 and 1,4-bis(2-methoxyethoxy)pillar[5]arene was obtained in a sufficient quantity for structural characterization and photostability study.

CC14, along with its precursors, were studied using NMR, UV-Vis and PL. The parent chromophore of CC14, which was also formed in the synthesis reactions for CC14, has a such a poor chemical stability that it was decomposed upon formation. Other dye chromophores were used for comparative photostability with CC14: 2-(3-cyano-4-((1E,3E)-3-(6-((E)-4-(diethylamino)styryl)-2',6'-dimethoxy-4,4-dimethyl-4,5-dihydro-[1,1'-biphenyl]-2(3H)-ylidene)prop-1-en-1-yl)-5-methyl-5-(trifluoromethyl)furan-2(5H)-ylidene)malononitrile (CC10) and 2-(4-((1E,3E)-3-(3-((E)-4-(bis(2-((tert-butyldimethylsilyl)oxy)ethyl)amino)styryl)-5,5-dimethylcyclohex-2-en-1-ylidene)prop-1-en-1-yl)-3-cyano-5,5-dimethylfuran-2(5H)-ylidene)malononitrile (CLD1).

CC14 is found to be more photostable than the benchmark chromophore CLD1 by nearly two orders of magnitude and a new version of CLD chromophore (CC10) by one order of magnitude. The result is exciting and stimulates new research toward development of extremely stable EO chromophores that may allow long-term operation of EO devices in air without the need for hermetic packaging which is expensive and technically challenging to do.

Chapter 1: General Overview of Organic Conjugated Molecules and Photostability

1.1 Organic Conjugated Molecules (OCMs)

Organic π-Conjugated Materials (OCMs) have π-electron conjugation along the main chain, with alternating single and double bonds. The large number of conjugated π-orbitals give these molecules some degree of semiconducting and optical properties: ease of electron propagation and absorption of the visible light. OCMs have been researched extensively, notably for uses in organic photovoltaics[1], electrooptic (EO) modulation[2,3], solid-state lasing[4,5], organic light emitting diodes (OLEDs)[6-8], biological imaging and sensing[9-12], chemical sensing[13-16] and ligands for photocatalysts[17-19].

Figure 1.1: Conjugated π-bonds shown in red

1.1.1 Conjugated Chromophores

Chromophores are colored pi-conjugated molecules and are found in azo dyes, biological pigments and food additives. Notable chromophores consist of biological pigments that have vibrant colors (lycopene and carotene) and porphyrin macrocycles (hemoglobin) [27,28]. During the mid to late 1800s research and development of colored compounds was being conducted. In 1856, a new dye, mauve, was discovered by Perkin. After characterization of this intensely blue colored dye, it was discovered to be a diazene dye. Also, many azo dyes were also discovered and synthesized, namely Para Red, one of the first fully synthetic dyes made by Meldola in 1885[91]. Chromophores are used in many

applications, from LCDs, imaging and data (CDs, DVDs, Blue-ray), dye sensitized solar cells, organic dye lasers and fluorophores.

When light is absorbed by the chromophore, π-electrons in the ground state are excited and moves to a higher anti-bonding orbital. Pi conjugation reduces the energy gap between the HOMO and LUMO level (HOMO is the highest occupied molecular orbital and LUMO is the lowest unoccupied molecular orbital). This in turn means light with a longer wavelength can be absorbed. In addition, presence of electron donors and acceptors can increase the degree of delocalization and reduce the HOMO and LUMO energy gap. For example, β-carotene is a highly conjugated dye found in certain vegetation and has absorption of 450-478nm, which appears yellow-orange in color. But when electron donors and acceptors are added to a conjugated system at the two opposite ends, much shorter conjugated linkage is needed to have absorption at the same or longer wavelengths. For example, streptocyanine is much shorter in conjugation length than that of β-carotene but has an absorption peak wavelength red-shifted to 519nm and perceives a reddish-purple color (See figure below). On the other hand, presence of aromatic units in the conjugated linkages (often called bridges) between donors and acceptors tend to shorten (blue-shift) absorption of chromophores. Other conceptual electronic and physical properties are described in the next section.

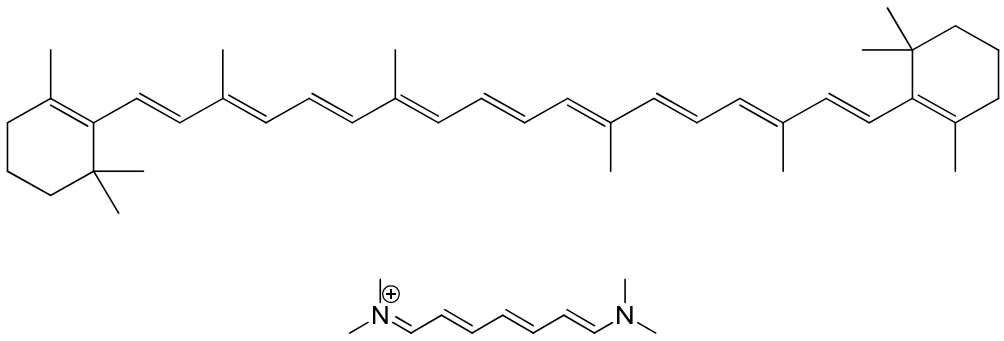

Figure 1.2: β-Carotene, an organic π-conjugated dye and streptocyanine, electron donor/acceptor

1.2 Electronic and Physical Properties of π-Conjugated Chromophore Molecules

Chromophores are characterized by the presence of extended pi-conjugated systems. The electronic properties of chromophores are mostly determined by pi-conjugated systems, of which the electronic structures are better described by the molecular orbital (MO) theory vs. the valence bond (VB) theory. Molecular orbitals can be divided into either bonding, anti-bonding or non-bonding orbitals. Where in a bonding orbital the electron density is between a pair of atoms causes attraction between the two nuclei and forming a covalent bond. Anti-bonding orbital has the electron density on the opposite side of each atom causing weakened interaction of the two nuclei, and dissociation occurs. Non-bonding orbitals do not contribute either positively nor negatively to the bond between two atoms.

Among all the molecular orbitals, HOMO and LUMO are the most important when optical and electronic properties of chromophores are considered. Energy levels of HOMO and LUMO are important in determining the energy gap between materials and whether they are insulating, conducting or semiconducting properties. In the language of

semiconductor, energy gap is often called bandgap, which refers to the difference in energy (eV) between the top of the valence band and bottom of the conduction band. HOMO is at the top of the valence band and LUMO is at the bottom of the conduction band. So, for electrons to move from valence to conduction band, some energy is required to transition. The energy can be the thermal energy or photon energy. The flow of current is determined by the electrons moving from valence to conduction band. Band gap is thus an important factor in determining conductivity. So, the difference in the energy of HOMO and LUMO determines whether a material has good charge carrier mobility or some degree of conductivity[30].

Larger band gaps are found in insulators, smaller band gaps are found in semiconductors. Conductors have very small band gaps or overlapping valence and conduction bands. Semiconductors do not absorb energy less than the band gap, so band gap can be probed by optical absorption measurement

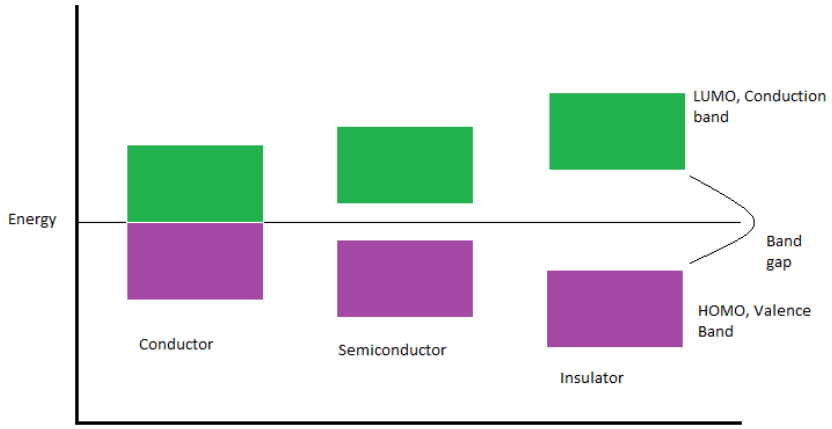

Figure 1.3: general bandgaps of conductors, semiconductors and insulators

Molecules and atoms have differences in the energy level transitions of electrons from one level to the next where the resultant effect is either emission or absorption of a photon. The energy of the photon is defined by E = hv. An excitation of an electron from HOMO to LUMO occurs only when the energy of the photon absorbed is equal to or greater than that of the band gap. Likewise, an already excited electron can spontaneously move to the ground state emitting a photon, a phenomenon called fluorescence. Phosphorescence, is another pathway where the absorbed photon does not relax, and it undergoes intersystem crossing to an excited triplet state.

Organic materials are structurally versatile and can be structurally modified. There are many effects to consider if altering the structure of the material. Growing the conjugated molecule by adding more alternating single and double bonds can affect the absorption of different wavelengths of light. As the number of conjugated bonds increases, the HOMO will increase and LUMO will decrease. The overall band gap decreases or narrows. Modifying the main structure can determine the need for donors and acceptors.

Donor and acceptor groups can increase or decrease overall electron density of the overall conjugated system plus affecting the band gap. Acceptors, which are electron deficient, pull electrons off the conjugated system lowering electron density. Lowering electron density, lowers LUMO energy level. This decrease is attributed to the decreased electron repulsion. Conversely, donors are electron rich groups that have high electron density where increasing electron density increases LUMO energy levels.

1.3 Photostability

The ability to withstand degradation of a conjugated molecule due to light is known as photostability. The photophysical phenomenon of molecular orbitals explains that as high-energy light hits a molecule, electrons can transition to other unoccupied molecular orbitals. This promotion of an electron weakens an existing bond and causes dissociation of the chemical bond due to the absorbance of light. So, photodegradation occurs when a material is exposed to light and its structural and physical properties are irreversibly altered by oxidation and hydrolysis [89,90]. Additionally, photodegradation in pharmaceuticals and drugs is another problem. Polymers and other organic molecules (dyes, for example) can be broken down due to UV light, form free radicals in the presence of oxygen and cleave carbonyl groups in the organic structure.

The extent of photodegradation can be analyzed from changes in absorbance and photophysical properties of the organic molecule and changes in chemical structures. The structural changes can be identified by UV-Vis absorbance, NMR, IR and other analytical instruments. UV-Vis absorption measures transitions from ground state to the excited state. NMR can characterize a wide variety of organic compounds by identifying neighboring protons, the number of protons and their respective environments. However, more than 1 mg is usually required to obtain a decent NMR spectrum, and photodegradation studies usually handle less than 1 mg of material. IR would more than likely be sufficient for measuring trace number of samples. Gas Chromatography (GC) and Liquid Chromatography (LC) with Mass spectrometry (MS) are good for smaller compounds but not good with larger organic conjugated molecules. Overcoming photodegradation can be beneficial for conjugated material devices and their applications,

but the main challenge is how to avoid the generation of and attach by reactive oxygen species.

1.3.1 Reactive Oxygen Species and Photodegradation Mechanism

Majority of photodegradation in OCMs occurs due to photooxidation by reactive oxygen species[31-35]. Notable examples of reactive oxygen species include peroxides, superoxide radical anions, hydroxyl radicals and singlet oxygen. Peroxides contain oxygen-oxygen single bond and are unstable in nature. Mechanistically, this single bond goes through homolytic cleavage and forms radical oxygen molecules. These peroxides can then oxidize other organic molecules and in principle can form during photodegradation.

Studies have shown that mechanisms that primarily affect OCMs involve mostly superoxide radical anions ($\cdot O_2^-$). These oxygen radicals are generated by light induced transfer of electrons from OCMs to oxygen molecules. Radical oxygen can abstract a hydrogen atom from α-carbon of alkyl chains thus producing a carbon radical, the oxygen radical can directly attack alkenes creating peroxide anions and carbon radicals. Thus, this radical degradation can affect side chains of OCMs and the main conjugated backbone.

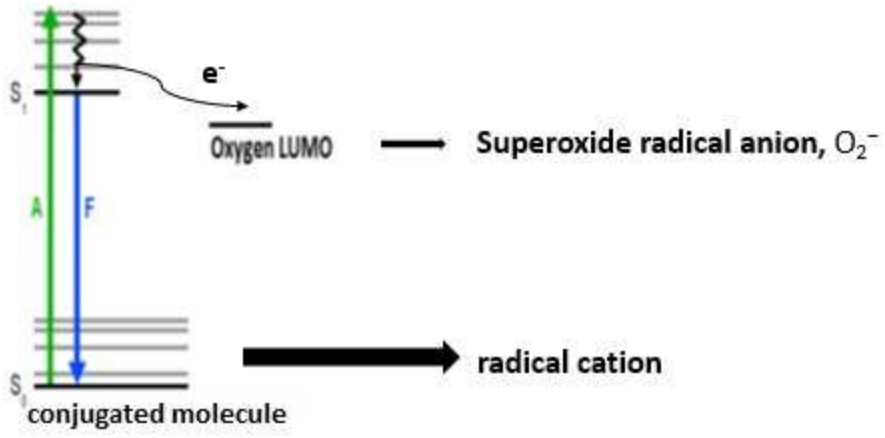

Figure 1.4. generation of superoxide radical anions by a reducing photoinduced electron.

Singlet oxygen species are another type of reactive oxygen species. Although they are to some extent less significant, they can still be formed. Normally, dioxygen is in its triplet state and cannot react with other organic molecules. But, the high energy singlet oxygen can react with organic molecules readily. The singlet oxygen is produced when energy is transferred from recently excited organic molecules to that of the triplet state dioxygen. These species can cause undesired cycloadditions of alkenes like 2+2 cycloadditions.

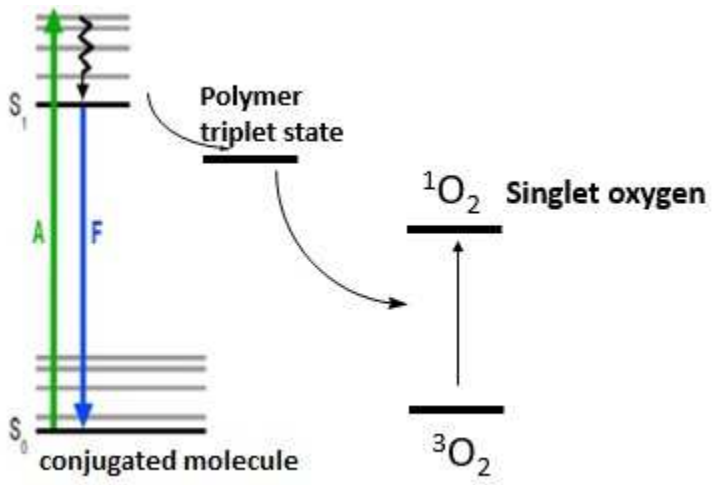

Figure 1.5: Generation of the singlet oxygen reactive species from the conjugate chromophore.

Radical degradation is usually much faster than the singlet oxygen degradation. Radical degradation is initiated when increased LUMO levels in a molecule, increase the occurrence of an electron being donated to another molecule with a lower LUMO level. So, there is a trend where LUMO energy levels and photostability are shown to be correlated. In other words, high LUMO levels indicate the OCM is less photostable. Side-chains and alkenes are easily affected by radical degradation, forming carbocations and peroxide anions. Singlet oxygen degradation affect non-aromatic alkenes by causing oxidative cycloaddition.

1.4 Strategies to Enhance Photostability

There are various methods and strategies found in literature that demonstrates and proposes ways to enhance photostability of OCMs. First, antioxidants [37], or singlet quenchers [38], added to OCMs can stabilize the polymer. This method is used for polymers (dyes), cosmetic and food [39,40]. The longevity of antioxidants is in question as they tend

to deteriorate after being consumed. Thus, they cannot provide long-term protection in devices and applications that require intense light.

Second, electron withdrawing groups can lower LUMO levels in OCMs thereby shutting down light induced electron transfer, preventing radical formation and improving overall photostability[33,36]. Photostability can be increased but reduction of LUMO levels alters optical and physical properties of the material. This phenomenon was observed in the synthesis of [poly(2,5-dialkoxyphenylenevinylene)] (RO-PPV)[41].

Third, synthetic pathways that make more resistant structures to singlet oxygen or oxygen radicals is another way to help photostability. Studies showed the use of dithienosilole instead of benzodithiopene[42] to prevent singlet oxygen attacks. Also, perfluorinated[43] and alkoxy[30] groups were used instead alkyl groups to combat oxygen radicals. Limited applicability is a result since the functionality of the material is altered. Last, controlling the triplet state energy by lowering is can potentially not excite oxygen to its singlet state. However, there is no method to control triplet state energy[44].

1.4.1 Alternative Solution to Enhance Photostability Via Encapsulation of Organic π- Conjugated Molecules

Encapsulation of organic π- conjugated systems is another method to increase photostability and is fundamentally different than the other proposed ideas aforementioned. Using a bulky material to sheathe the π- conjugated system, one can prevent oxygen from reaching the π- conjugated system. This is seen in flurophores[73-75] and proteins [76]. Initial nano particle encapsulation has been used for fluresence imaging and sensing.

Encapsulation has been performed at a molecular level in the form of rotaxanes [46-51]. Although many rotaxane structure were proposed (see chapter 2), only a few were specifically designed with photostability in mind. Photostability enhancement was seen in alpha- and beta- cyclodextrin[58,59], cucurbituril[56], and a squarine dye in a tetra amide macrocycle [77]. The encapsulation, however, is not tight enough to exclude oxygen in structures discussed in section 2.1.1 and are very specific for certain cationic chromophores and other cationic precursors [56,58,59, 77-79].

In this research, synthesis of pillar[5]arene encapsulated chromophore is explored and the photostability of encapsulated chromophores is compared with the benchmark EO chromophores to determine the effectiveness of molecular encapsulation on photostability.

Chapter 2 General Overview of Encapsulation and Design of Chromophores Encapsulated with Pillar[5]arenes

2.1 Host-Guest Chemistry

Host-guest chemistry is an important facet in supramolecular chemistry[45]. These complexes are composed of two or more molecules or ions that are held together based on molecular level interactions (hydrogen bonding, van der Walls forces, ionic bonding or polar interactions) rather than covalent bonds. Non-covalent like this is seen in proteins and involved in many biological processes in which large molecules bind specifically to a certain molecule or ion—but not permanently. Common host molecules include cyclodextrins, calixarenes, pillarenes and cucurbiturils.

2.1.1 Rotaxanes and Other Large Macrocylic Molecules

Rotaxanes are important since the chemistry and the principles behind the encapsulation are important [46-51]. Rotaxanes have an interlocked molecular structure where part of the molecule is the "thread" and is threaded through or encapsulated by a macrocycle (a large molecular complex with a cavity). Then the threaded molecule is capped on either side preventing the macrocycle from dissociating or "slipping out". Some rotaxane like structures are naturally present in peptides like the cystine knot peptide[52]. This type of complex formation is known as host-guest chemistry.

Calixarenes are a type of macrocycle capable of holding small ions and molecules in its basket-like cavity, due to the cavity having hydrophobic properties. The large cone molecule can complex with ions just as cadmium and lead. Additionally, they can be

used for ion sensitive electrodes and sensors. Although, not much progress has been made using calixarenes for photostability studies [53].

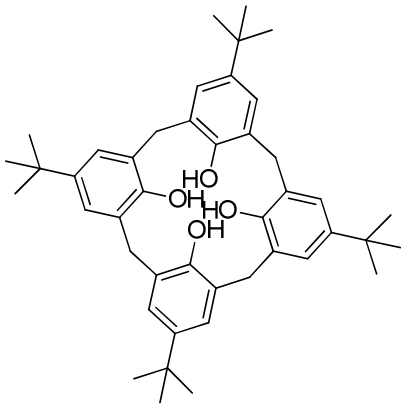

Figure 2.1: Calix[4]arene structure, the most basic form

Cucurbiturils are another type of macrocycle that is synthesized via glycoluril monomers and methylene bridges. The oxygen molecules of the complex curve inwards creating a pumpkin-like structure that gives the cavity formed a high affinity of cationic molecules. Cucurbiturils have been used as macrocycles for rotaxane assembly, where hexamethylene diamine was used as the guest molecule[54]. Cucurbiturils are also used as drug delivery systems where oxyplatin is the guest molecule and a larger cucurbit[7]uril as the host[55]. However, a few have been few cucurbiturils used for photostability enhancement[56].

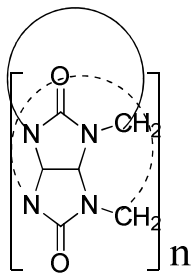

Figure 2.2: Generic cucurbit[n]uril structure

Cyclodextrins are cyclic oligosaccharides that are yet another macrocycle that has host-guest properties. Cyclodextrins are composed of more than 5 α-D-glucopyranoside that have 1->4 glyosidic linkages. Moreover, these complexes are water soluble with a hydrophobic cavity and hydrophilic exterior. There are 3 common cyclodextrin molecules all of which are sugar ringed complexes that form a cone shape: α-cyclodextrin (6 cyclic sugars), β-cyclodextrin (7 cyclic sugars), and γ-cyclodextrin (8 cyclic sugars). Other larger cyclodextrins have been synthesized but their uses and stability are low. Cyclodextrins have mainly used in food, drug delivery and aerosols. Plus, cyclodextrins have been used as macrocycles for rotaxane assembly using g-cyclodextrin[54,57]. There have been a few instances of cyanide dyes used with α- and β-cyclodextrin for photostability studies [58,59].

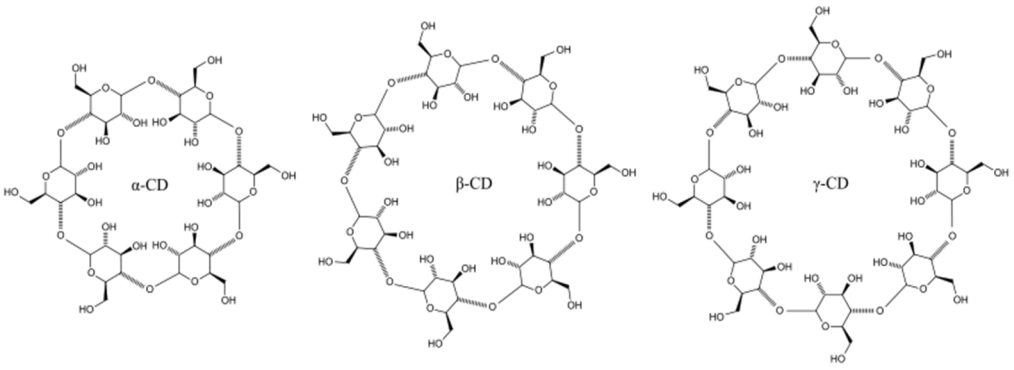

Figure 2.3: Three major types of cyclodextrins.

As mentioned earlier, MLE has been reported mostly for cationic and azo dyes. Although a neutral-core chromophore has been encapsulated in cyclodextrin,[60] the reaction was done in water to take advantage of hydrophobicity of chromophore core but requires water solubility for the precursors, and thus has limited applicability. In addition, other macrocycles are lacking in some regards compared to the pillar[5]arene structure.

Calixarenes and cyclodextrins have cone-like structure where the end with larger opening may not provide effective shielding of chromophore. Cucurbituril cannot be derivatized due the glycoluril structure, hence affecting solubility. Pillar[n]arenes are a relatively new class of macrocycle molecule [60-70]. The encapsulation of guest molecule via pillar[5]arenes can prove to be advantageous because it can prevent the guest molecules from undergoing photodegradation via light or oxygen.

2.2 Brief Overview of Pillar[5]arenes

Pillar[5]arenes are large macrocyclic molecules composed of varying numbers of hydroquinone units (5-10) linked via methylene bridges at the para- position. Structurally Pillar[5]arenes are like cucurbiturils and calixarenes. The 1,4-dimethoxypillar[5]arene was first synthesized by Ogoshi et al. (2008) and is composed of 5 hydroquinone subunits [67].Pillar[5]arene is the most common and stable among other Pillar[5]arene structures. These new macrocycles were named pillar[5]arenes since they resembled a cylindrical pillar composed of aromatic molecules. These structures were created to primarily to study supramolecular chemistry. Additionally, derivatives of the pillar[5]arene structure can be generated by modifying at 1- and/or 4- hydroxyl positions.

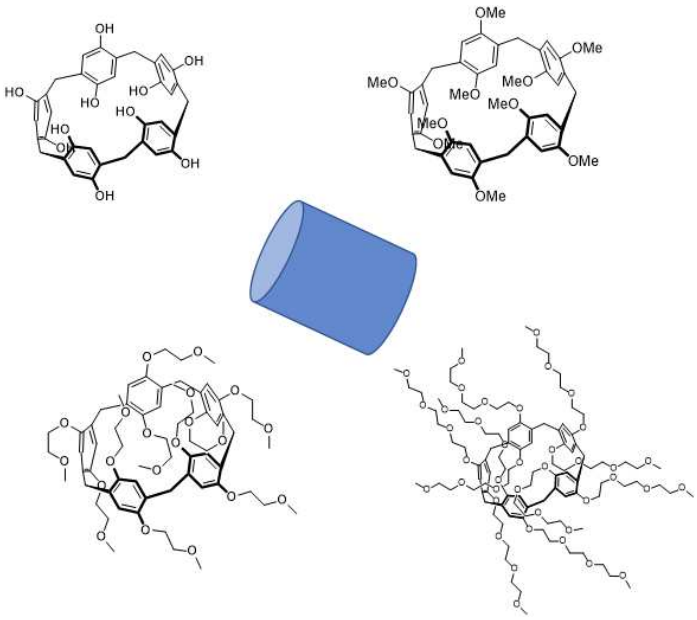

Figure 2.4: Types of pillar[n]arenes and its cylindrical structure

Pillar[n]arenes have a symmetrical cylindrical structure that has two openings with an electron rich cavity. The cavity can potentially pair well with electron poor groups (guests) and the pillar[n]arene (host) can accept these guests due to the electron rich environment. Moreover, the large complex of the pillar[n]arene can protect groups within its cavity, protecting groups from photodegradation.

Synthesis of pillararenes, namely pillar[5]arene is mainly through thermodynamically controlled Friedel-Crafts alkylation[68]. The reaction generally occurs when a mixture of 1,4- dimethoxybenzene and formaldehyde is treated with trifluoracetic acid as the Lewis acid at room temperature. pillar[6]arene can be synthesized by using the similar Friedel-Crafts alkylation, however; bulky alkoxy groups, bulky chlorinated solvents and different Lewis acids must be used[69]. Additionally, homologous ring expansion of pillar[5]arene can yield higher pillar[5]arenes ($n > 6$), but

these larger pillar[5]arene structures are not currently explored due to low yield and difficulty of synthesis[70].

The flexible supramolecular container molecule provides adequate protection of both ends of the molecule and can be structurally modified. Ogashi group has done a lot of work in the construction of rotaxanes of aliphatic polymers [61,62]. Other cationic structures were also synthesized such as alkylpyriridinium and viologen [63-67]. Other known applications include biomedical applications, where carboxylated pillar[5]arene forming host-guest complexes can show potential for drug delivery using mematine [71]. Last, pillar[5]arene have shown potential applicability as organic light emitting materials[72].

2.3 Research Overview and Goals

The goal of this research is to develop an effective site- based isolation by using molecular level encapsulation (MLE) to protect sensitive EO chromophore molecules from photo-oxidation. This is needed for applications that require operation under intense light: electro-optic waveguide devices [80], dye lasers[81], and optical oamplifies[82]. Electro-optical (EO) chromophores[83] will be used to improve encapsulation efficiency and overall yield of product, additionally, study the effects of photostability enhancements for potential optoelectric applications. Additionally, encapsulation will help reduce issues such as dipole-dipole interchromophore interactions that can cause aggregation of the chromophore molecules. Although, molecular encapsulation to protect π- conjugated molecules and improve stability is not necessarily a novel concept. The research does, however, have novel methods and ideas not employed before.

In general chromophores have three major units: the electron donors, the organic π- conjugated backbone and an acceptor molecule[84, 86-88]. Having a conjugated system with both donor and acceptor creates a structure that is both electronically asymmetrical and polarizable. Synthesizing chromophore precursors is the first stage in this research. The first precursors synthesized has electron donating properties and is very bulky in nature, which makes it stopper A (see figure below). Starting from **2,2,6,6-tetramethylpiperidine** then going to **4-(2,2,6,6-tetramethylpiperidin-1-yl) benzaldehyde** is the first stage of having the bulky donor with a reactive aldehyde group, which can be extended to form a donor-bridge structure **(2E,4E,6E)-7-(4-(2,2,6,6-tetramethylpiperidin-1-yl)phenyl)hepta-2,4,6-trienal**. **2-(3-cyano-4,5-dimethyl-5-(trifluoromethyl)furan-2(5H)-ylidene)malononitrile (CF_3-TCF)** is then used as the acceptor to couple with the aldehyde. CF_3-TCF are good electron acceptors that increases hyperpolarizability in chromophores[85]. The molecules will be in solution and will self-assemble, adding the encapsulating molecule, pillar[5]arene, with the acceptor and π-conjugated backbone.

For the molecular level encapsulation (MLE) of the chromophore, the cylindrical Pillar[5]arene molecule will be used. **1,4-dihydroxypillar[5]arene** will be synthesized based on the procedure of Ogashi et al. [67] The hydroxy version of pillar[5]arene will be modified with two different groups to give 1,4-bis(2-methoxyethoxy)pillar[5]arene and **1,4-bis(2-(2-(2-methoxyethoxy)ethoxy)ethoxy)pillar[5]arene**.

Successful encapsulation requires that the polyene part of the donor-bridge can thread into the cavity of the pillar[5]arenes. Among charge neutral structures, alkane chains have been reported to form rotaxanes with pillar[5]arenes. Complexation of the

donor-bridge with the pillar[5]arenes is possible due to pi-pi interaction between the polyene and the phenylene units of the pillar[5]arene, and can be readily confirmed by NMR study of the solutions of the donor-bridge and the pillar[5]arenes.

Molecular level encapsulation (MLE) is shown schematically in Figure 2.5. A chromophore precursor will be designed and synthesized with a bulky structure (stopper A) at one end and a reactive group at the other side of the chain (typically an aldehyde). The chromophore precursor with stopper A will self-assemble within the cylindrical pillar[5]arene molecule as a guest molecule and subsequently be capped by an acceptor molecule (stopper B) at the reactive end forming a molecularly encapsulated chromophore (MEC) as the final rotaxane-like product.

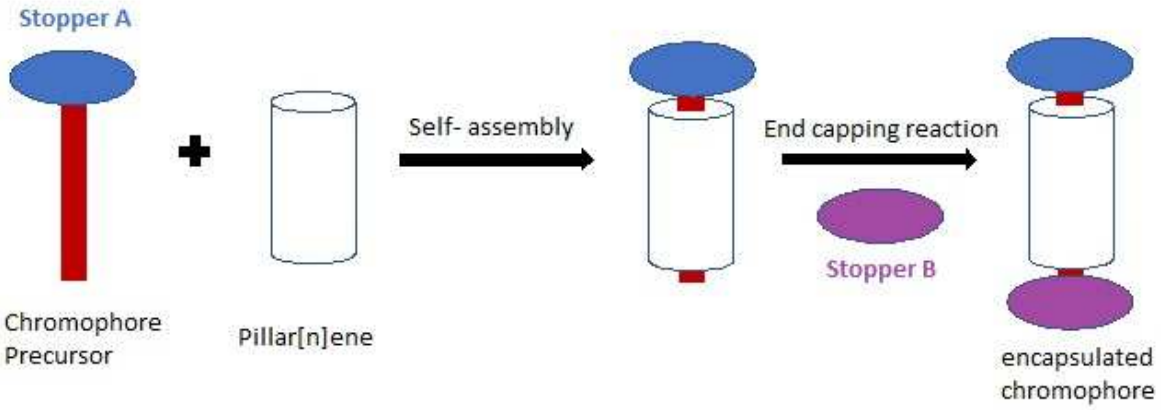

Figure 2.5: Simple scheme illustrating encapsulation on a molecular level

Chapter 3 Experimental

3.1 Materials and Methods

The nitrogen filled glovebox was used for many steps. All other glassware and column that were used were purchased from Fisher Scientific. The NMR data that was collected using Bruker Avance 400MHz and 600MHz NMR instrument. UV-vis spectra were obtained from Agilent 8453 photodiode array spectrometer. The photoluminescence studies were conducted using Perkin Elmer LS-50B luminescence spectrometer. The measurements were done in air and nitrogen. For the photostability study, a Newport light source (model 66903) with a 300 W xenon arc lamp and a Newport power supply (model 69911) was used. The light intensity can be adjusted using a Newport 70260 power meter and the unit intensity is 2200-2600mM/cm^2, which is > 20 times the sun's intensity. The photostability was tested in air using film samples coated on quartz substrates under a white light intensity of 1.24 W/cm^2 or 12.4 standard sun.

Each of the three starting materials (the donor-bridge, acceptor, and pillar[5]arene) was synthesized in multiple steps. 2,2,6,6-tetramethylpiperidine (TMP) was chosen as an electron donor for the ease of its incorporation and its ability to serve as a stopper (as its size is greater than the cavity of pillar[5]arenes, ~ 5Å).

3.1.1 Donor, Acceptor And Pillar[5]Arene Synthesis

Pillar[n]arenes are the major structure used to encapsulate the conjugated polymers. First, the methoxy version of pillar[5]arene was synthesized using the schematic found below.

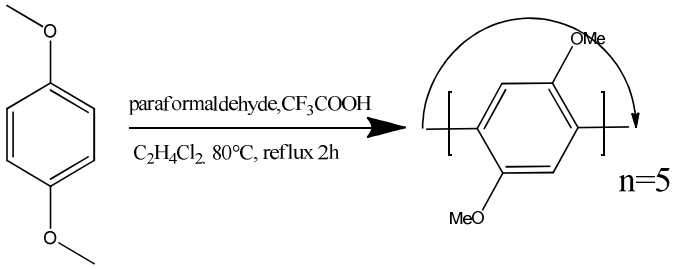

Scheme 1: Synthesis of 1,4-dimethoxypillar[5]arene

1, 4-Dimethoxypillar[5]arene

7.00 g of 1,4- dimethoxybenzene, 1.75 g paraformaldehyde, 250 mL 1,2-dichloroethane, 15 mL trifluoracetic acid was added to 500 ml round bottom flask. The reactants were left to react at 80 ^{o}C under reflux for 2 hrs. The white precipitate was collected in methanol, and then the methanol was evaporated to get the solid precipitate. The solid product was then dissolved in a chloroform/acetone mixture (1:1). Column chromatography was done using chloroform and ethyl acetate (~99:1). The yield received was 30%. There was water present also about 30%. ^{1}H NMR (400 Mz, $CDCl_3$): δ ppm (6.84) (s, 10H, Phenyl), 3.76 (s, 10H, methylene), 3.71 (s, 30H, methoxy).

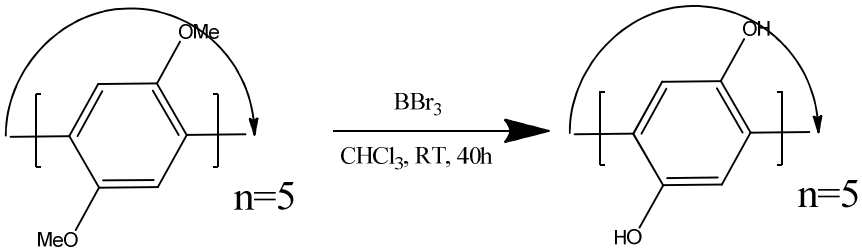

Scheme 2: Synthesis of 1,4-dihydroxypillar[5]arene

1,4-Dihydroxypillar[5]arene

The reaction was done at room temperature. In a 250 mL flask, 3.15g 1,4-dimethoxypillarene, 100 mL of chloroform, 4.03 mL of boron tribromide was added. A room temperature water bath was prepared since the reaction was slightly exothermic (~30 ^{o}C). Reaction was stirred for 40 h. The flask was cloudy white. The contents were filtered, and the white solid was added to 100 mL of water and left overnight. The solution was slight brown in color. The solution was boiled for 5 mins then the solid was filtered, washed with DI water and air dried. The solid was added to 50 mL of THF and stirred for a few hours. The THF was removed via vacuum. Yield= 28%. ^{1}H NMR (400 Mz, DMSO-d6): δ ppm 8.46 (s, 10 H, OH), 6.59 (s, 10H), 3.45 (s, 10H).

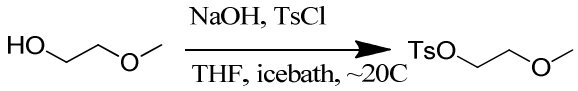

Scheme 3: Side-chain synthesis of 2-methoxyethyl tosylate

2-Methoxyethyl tosylate

This precursor was synthesized for modification of pillar[5]ene for better solubility. In the glove box, to a 250-mL round bottom flask, 4.5 g of NaOH (powder), 40 mL of anhydrous THF, and 7.25 g of 2-methoxyethanol were added and then 18.52 g of tosyl chloride was added slowly. Flask was taken out of the glove box and cooled in an ice bath. The flask was stirred for 5 mins and then swirled by hand as the mixture became to viscous to stir. 2mL of acetic acid was added. The precipitate was filtered. THF was aired off. The residue was dissolved in diethyl ether. Potassium carbonate was added until solution was neutral. Then, magnesium sulfate was added to dry product. After

filtration to remove the solid, the solution was distilled on a rotary evaporator to afford the product. Yield: 30%. ^{1}H NMR (400 MHz, $CDCl_3$): δ (ppm) 7.75 (d, 2H, aryl), 7.46 (m, 2H, aryl), 3.70-3.65(t, 2H, J=7.5Hz, CH_2), 3.56-3.49(t, 2H, J=7.5Hz, CH_2), 3.30 (s, 3H, CH_3), 2.34 (S, 3H, CH_3)

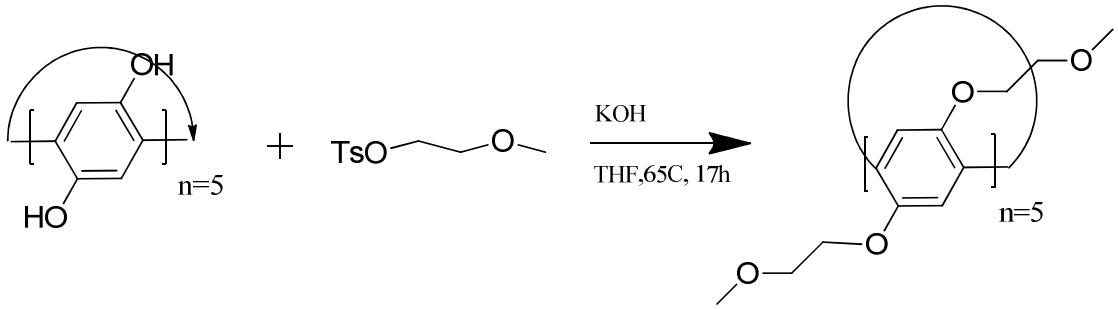

Scheme 4: Synthesis of 1,4-bis(2-methoxyethoxy)pillarene

1,4-Bis(2-methoxyethoxy)pillarene

The reaction was setup in the glovebox then removed after contents were added. To a 50 mL flask were added 1,4-dihydroxypillarene (0.55 g, 1 mmol), 2-methoxyethyl tosylate (1.61 g, 7 mmol), THF (7ml) and KOH powder (10 mmol, 56.1 g). The flask was heated at 65 ^{o}C for 60 h while stirring. The solvent was then removed via filtration. Reaction was worked up using dilute HCl (0.2 M). The brown solid was then separated via silica gel column chromatography. Ethyl acetate/hexane (2:1) was used as the eluent. Product appeared after a few bands had been collected. Product was light pink in color. ^{1}H NMR (400 MHz, $CDCl_3$): δ (ppm) 6.88 (s, 10H, aryl), 4.02 (t, J=5.01 Hz, 20H, CH_2), 3.78 (s, 10H, methylene), 3.69 (t, J=5.00Hz, 20H, CH_2), 3.36(s, 30H, CH_3).

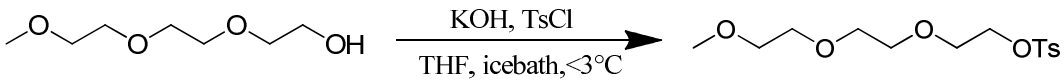

Scheme 5: Side-chain synthesis of 2-(2-(2-methoxyethoxy)ethoxy)ethyl 4-methylbenzenesulfonate

2-(2-(2-Methoxyethoxy)ethoxy)ethyl 4-methylbenzenesulfonate

In the glovebox, NaOH (1.5 g, 36 mmol), triethylene glycol monomethyl ether (4.25 g, 26 mmol) and tosyl chloride (4.75g, 25 mmol) was slowly added in a flask. The reactant flask was then taken out of the glovebox and placed in an ice bath for 5 mins. The reaction was slightly exothermic, and the temperature was maintained at < 3°C. Acetic acid (1 mL) was then added to the flask and reaction was stirred for another minute. The THF was then removed and the precipitate was filtered. There was lot of water present so 3ml of ether was added and the organic layer extracted. Magnesium sulfate was then used as the drying agent. Then the organic liquids were vacuumed at 60 °C for 5 mins to receive the oil. Yield: 20.1%. ^{1}H NMR (400 Mz, $CDCl_3$): δ (ppm) 7.8 (d, 2H, aryl), 7.35 (d, 2H, aryl), 4.16 (t, J=4.8Hz, CH_2), 3.72-3.50 (m, 10H, CH_2), 3.37 (s, 3H, CH_3), 2.45 (s, 3H, CH_3).

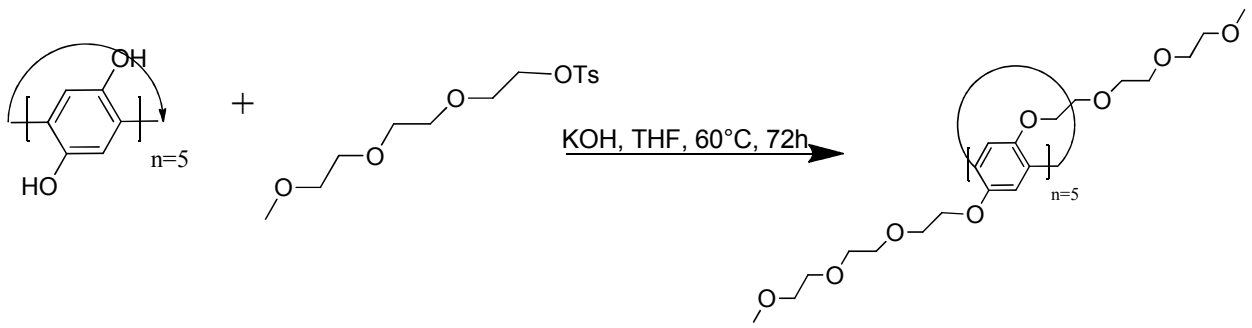

Scheme 6: Synthesis of 1,4-bis(2-(2-(2-methoxyethoxy)ethoxy)ethoxy)pillar[5]arene

1,4-Bis(2-(2-(2-methoxyethoxy)ethoxy)ethoxy)pillar[5]arene

In the glovebox, to a 50 mL flask were added 1,4-hydroxypillar[5]ene (0.6 g, 1 mmol), 2-(2-(2-methoxyethoxy)ethoxy)ethyl 4-methylbenzenesulfonate (2.25 g, 7 mmol), THF (7 mL), powdered KOH (0.56g, 10mmol). The flask was heated in an oil bath at 65C for 40 hrs. The THF was removed. The reaction mixture was neutralized with dilute HCl (2N, 2 mL). The mixture was extracted with diethyl ether, and the extract was dried with sodium carbonate. After removal of the ether, a brownish oil was obtained. The crude product was purified on a silica gel column Ethyl acetate was used as the first eluent, then was switched to acetone. Yield: 2.4%. ^{1}H NMR (400 Mz, CDCl3): δ (ppm) 6.83 (s, 10H, phenyl), 4.01-3.97 (m, 20H, CH_2), 3.83 (t, J=4.8Hz, 20H, CH_2), 3.74-3.72(m, 30H, CH_2), 3.66-3.64(t, J=4.7Hz, 20H), 3.60-3.58 (m, 20H, CH_2), 3.47-3.45(m, 20H, , CH_2), 3.28 (s, 30H, CH_3). There were a few solvent peaks and an unknown peak at 1.5.

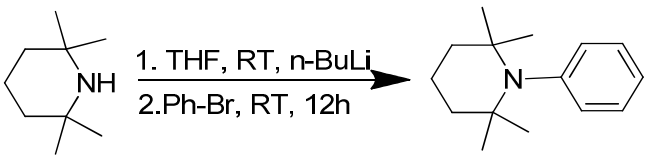

Scheme 7: Synthesis of donor 2,2,6,6-tetramethyl-1-phenylpiperidine

2,2,6,6-Tetramethyl-1-phenylpiperidine

In the glovebox, a 250 mL flask was used and the following 6 g 2,2,6,6-tetramethylpiperidine, 11 mL of THF, 16 mL of n-BuLi (2.5 M) was added over few minutes. The flask was sealed. 3 g of bromobenzene/10 mL of THF was added via needle and syringe. Reaction was stirred for 12 hrs at RT. THF was removed via vacuum distillation at 70 °C. Then column chromatography was done. ^{1}H NMR (400 Mz, CDCl3): δ (ppm) 7.26-7.18 (m, 5H, phenyl), 1.75-1.69 (m, 2H), 1.58-1.53 (m, 4H), 1.01 (s, 12H).

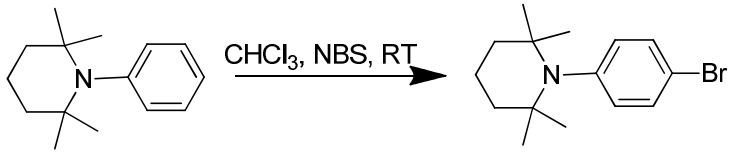

Scheme 8: Synthesis of donor 1-(4-bromophenyl)-2,2,6,6-tetramethylpiperidine

1-(4-Bromophenyl)-2,2,6,6-tetramethylpiperidine

In the glovebox, to a 250-mL flask were added 1.6 g of 2,2,6,6-tetramethyl-1-phenylpiperidine, 15 mL of chloroform and 1.43 g of NBS. The flask was placed in a water bath and stirred for 30 mins at RT. Chloroform was removed. Hexane was added to extract the product. The hexane solution was then condensed to obtain an oil. ^{1}H NMR (400 Mz, CDCl3): δ (ppm) 7.37 (d, J= 8.5Hz, 2H, phenyl), 7.08 (d, J=8.6 Hz, 2H), 1.69-1.72 (m, 2H), 1.56-1.52 (m, 4H), 0.99 (s, 12H).

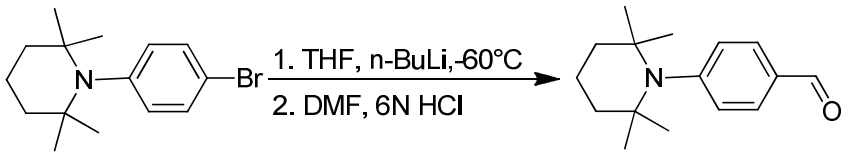

Scheme 9: Synthesis of donor 4-(2,2,6,6-tetramethylpiperidin-1-yl)benzaldehyde

4-(2,2,6,6-Tetramethylpiperidin-1-yl)benzaldehyde

To a flask, 5.5 g of 1-(4-bromophenyl)-2,2,6,6-tetramethylpiperidine, 25 mL of THF and 8 mL of n-BuLi (2.5 M) was slowly added. The flask was placed in a ~ –59 ºC dry ice/ ethanol (70% v/v) bath. After formation of white solid, dimethylformamide (1.54 g) was added. Reaction was run for 30 mins and was then treated with 6 N HCl (7.2 mL) to reach pH 6. THF was removed by air. Hexane was added for extraction. Magnesium sulfate was used as the drying agent. The oil product was purified using column chromatography using ethyl acetate/ hexane (1:45) as the eluent. Yield: 14%. ^{1}H NMR (400 Mz, CDCl3): δ (ppm) 10.00 (s, 1H, aldehyde), 7.81 (d, 2H, J=8.5Hz, phenyl), 7.38 (d, 2H, J=8.3Hz, phenyl), 1.78-1.71(m, 2H), 1.6-1.54 (m, 4H), 1.03 (s, 12H).

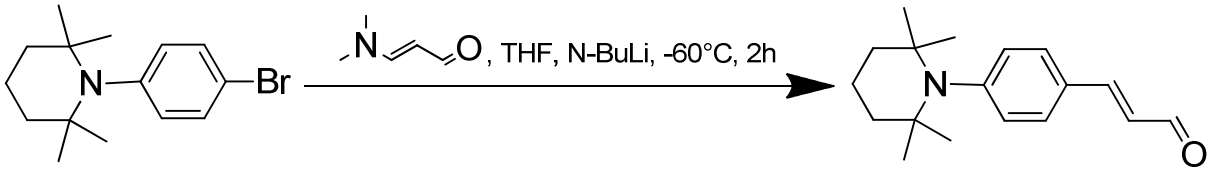

Scheme 10: Synthesis of DB1

(E)-3-(4-(2,2,6,6-tetramethylpiperidin-1-yl)phenyl)acrylaldehyde (DB1)

First, a cooling bath was prepared using dry ice/ethanol (70% v/v) the temperature was monitored using an electronic thermometer (~ –60 °C). Then, in the glovebox, 1-(4-Bromophenyl)-2,2,6,6-tetramethylpiperidine (2.1g, 7 mmol), THF (10 mL), and 3-(dimethylamino)-2-propenal (0.75, 7.3 mmol) was added to the 250-mL flask and sealed with rubber stopper. Using a needle and syringe, N-BuLi (3 mL, 2.5M) was added to the flask slowly. The flask was then removed from the glovebox, placed in the cooling bath. While stirring dilute HCl (2N, 4 mL) was added. Contents stirred for 2 hrs. Next, THF was removed. Hexane was added for extraction. NaOH added to neutralize acid. The murky precipitate was collected via filtration. Column chromatography done using ethyl acetate/ hexane (1:25). Initial bands contained starting material and side reactions. Last few bands contained notable amount of product. Yield: 15.6%. ^{1}H NMR (400 Mz, CDCl3): δ (ppm) 9.71(d, J=7.8Hz, 1H), 7.5-7.46(m, 3H), 7.28-7.26(m, 2H), 6.72(d, J=7.6Hz, 1H), 1.78-1.70(m, 2H), 1.58-1.54(m, 4H), 1.03(s, 12H).

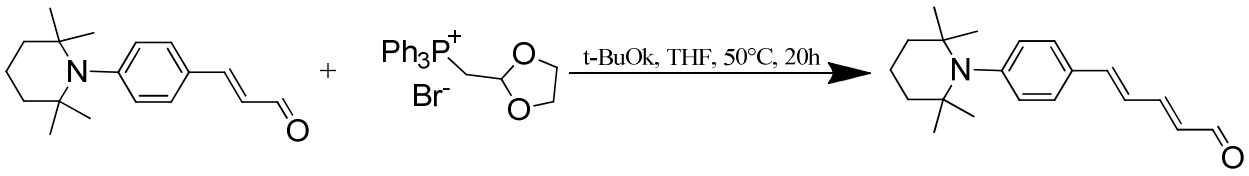

Scheme 11: Synthesis of DB2

(2E,4E)-5-(4-(2,2,6,6-tetramethylpiperidin-1-yl)phenyl)penta-2,4-dienal (DB2)

((1,3-dioxolan-2-yl)methyl)triphenylphosphonium bromide (1.1 g, 2.6 mmol), 10 mL of THF, t-BuOK (1.25 g, 11.1 mmol) and (2E,4E)-5-(4-(2,2,6,6-tetramethylpiperidin-

1-yl)phenyl)penta-2,4-dienal (0.58 g, 2.13 mmol) were added to a 250-mL flask in the glovebox. Then the sealed flask was heated (50 °C) and stirred for 20 hr. The THF was removed. Acetone (10ml) and dilute HCl (2 N, 4 mL) were added. The solution was stirred for 1 hr. Sodium carbonate was added to neutralize acid. Acetone was removed, and the precipitate was collected via filtration. Separation done via column chromatography using ethyl acetate/hexane (1:20) as the eluent. Initial bands contained starting material with trace product. Majority product collected near middle band. Yield: 15.4%. ^{1}H NMR (400 Mz, CDCl3): δ (ppm) 9.62 (d, J=8Hz, 1H), 7.46-7.36 (m, 2H), 7.30-7.20 (m, 4H), 7.00-6.94 (m, 2H), 6.28 (q, J=8Hz, 1H), 1.76-1.72 (m, 2H), 1.56 (t, J=6 Hz, 4H), 1.02 (s, 12H).

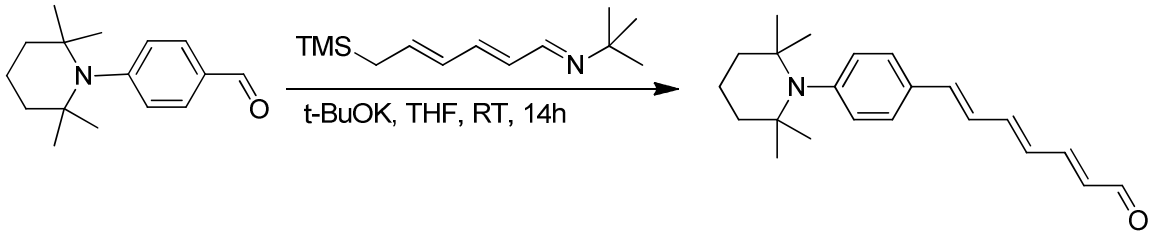

Scheme 12: Synthesis of DB3

(2E,4E,6E)-7-(4-(2,2,6,6-tetramethylpiperidin-1-yl)phenyl)hepta-2,4,6-trienal (DB3)

4-(2,2,6,6-tetramethylpiperidin-1-yl)benzaldehyde (1.652 g, 6.73 mmol), (E)-2-methyl-N-((2E,4E)-6-(trimethylsilyl)hexa-2,4-dien-1-ylidene)propan-2-amine (1.22 g), t-BuOK (0.765 g) was added in the glovebox at RT and stirred for 1 h. Small amount of acetic acid was added to flask to adjust the pH to 3-4. Then the mixture was stirred for 15 h. THF aired away, then ether and aq. sodium bicarbonate were added. The extract was

condensed and purified using column chromatography. Eluent used was ethyl acetate/ hexane (1:45). The product was crystallized in hexane to give orange red crystal. Yield: 10.5%. ^{1}H NMR (400 Mz, $CDCl_3$): δ (ppm) 9.6 (d, J=8Hz, 1H), 7.36-7.34 (m, 2H), 7.26-7.16 (m, 3H), 6.88-6.80 (m, 3H), 6.62-6.52 (m, 1H), 6.22-6.13 (m, 1H), 1.76-1.68 (m, 2H), 1.6 (t, J=6Hz, 4H), 1.02 (s, 12H).

3.1.2 MLE of Acceptor, Donor-Bridge and Pillar[5]arene

Schemes 13-17 show the reactions done for chromophore encapsulation (See table below).

	Donor Bridge	Pillar[5]arene	Acceptor	Reaction condition	Product
13	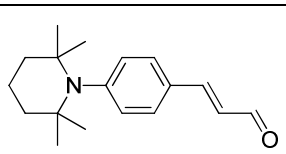	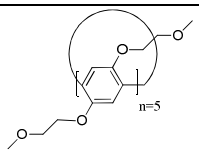	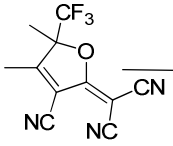		No product
14	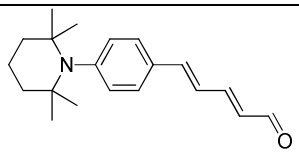	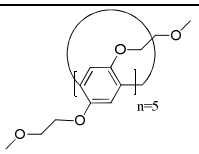	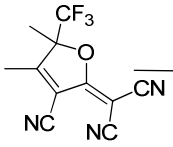		CC14
15	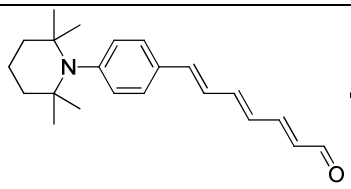	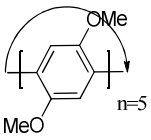	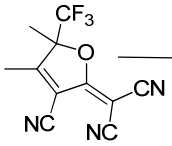		Low yield, CC15
16	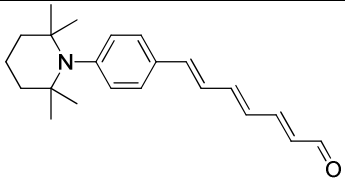	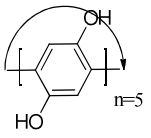	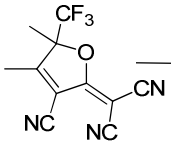		No product

17	

Figure 3.1: Schemes 13-17 of MLE reactions

In scheme 13-14, and 16-17 the reactions did not bode well as lot of the reactants were not miscible and after conducting TLC it was discovered no new compound was present. During the reactions, most likely the chromophore had degraded before encapsulation. Lot of side products and unknown compounds were discovered when these final MECs were attempted to be synthesized. Only one MEC gave reasonably good yield, CC14.

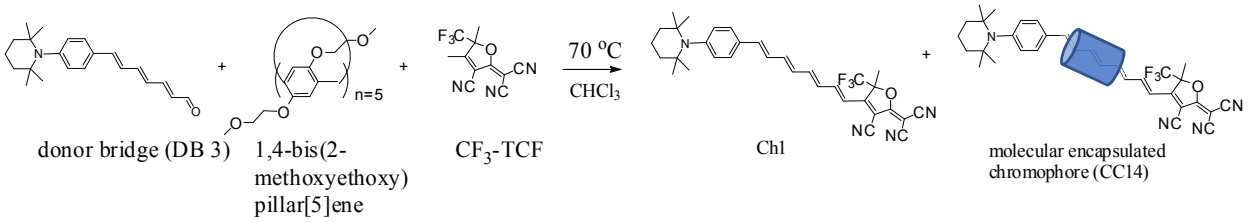

Scheme 18: Synthesis of CC14 and side product Ch1. The blue cylinder represents the 1,4-bis(2-methoxyethoxy)pillar[5]arene encapsulation.

A mixture of 1,4-bis(2-methoxyethoxy)pillar[5]arene(2.24 g), DB3 (0.51 g), CF_3-TCF (0.44 g) and $CHCl_3$ (0.223 g) in a vial was heated to dissolve the reactants. The chloroform was then removed by evaporation under heating. The vial was closed and heated for 60 h at 70°C. The solid was taken up using chloroform and purified on a silica gel column using EtOAs/hexanes (1:3 v/v) as the eluent. Yield: 260 mg, 9.4%. ^{1}H NMR (400 Mz, CDCl3): δ (ppm) 7.61 (m, 1H), 7.38(d, J=7.8Hz, 1H), 7.26 (m, 2H), 6.95 (s,

6H), 6.63-6.53(m, 1H), 5.89-5.75(m, 1H), 4.93-4.86 (m, 1H), 4.04-3.99 (m, 3H), 3.96-3.91 (m, 4H), 3.88 (s, 5H), 3.76 (s, 12H), 3.54 (s, 6H), 3.44-3.35(m, 18H), 1.99 (s, 3H), 1.78-1.73(m, 2H), 1.63(s, 3H) 1.10(s, 9H). One thing to note: CC14 was surprisingly stable on a TLC plate, clearly indicating that TMP and the acceptor are effective stoppers.

Chapter 4 Results and Discussion

4.1 NMR Analysis of Donor-Bridges, Acceptor, Pillar[5]arenes and Encapsulated Chromophores

The donor bridge is shown in scheme 17 and Figure 4. Each of the three starting materials (the donor-bridge (DB3), acceptor (CF_3-TCF), and 1,4-dihydroxypillar[5]arene) was synthesized in multiple steps. 2,2,6,6-Tetramethylpiperidine (TMP) was chosen as an electron donor for the ease of its incorporation and its ability to serve as a stopper (as its size is greater than the cavity of pillar[5]arenes, ~ 5Å). Synthesis of encapsulated chromophore is very challenging. It was found that reactions performed in a solvent never yield any meaningful amount of product. This is because of the lack of specific (or strong) interaction between donor-bridge and the cavity of pillar[5]arene. Success was only achieved in solid state reaction. However, solid state reaction requires the formation of solid solution of all reactants. Some reactants such as methoxy and hydroxy versions of pillar[5]arene (in Schemes 15 and 16) are highly crystalline and could not form a solid solution with other reactants, and thus afforded practically no product.

The length of the bridge also determines the success of encapsulation. Shorter conjugated donor bridges (DB1 and DB2) in Scheme 13 and 14 did not lead to encapsulated chromophore likely due to the insufficient length of the bridges. The

reaction in Scheme 17 was conducted in methanol and a very small amount of blue chromophore was obtained. The amount was not enough for NMR characterization. Further investigation of the reaction is needed.

The reaction in scheme 18 was explored the most intensively, and the best yield obtained was 9% from a solid-state reaction at 70 ^{o}C. This allowed us to synthesize sufficient amount of the encapsulated chromophore, CC14, for optical and NMR characterization, and photostability testing.

Complexation of donor-bridge and pillar[5]arene in solution: All precursors of CC14 were mixed in $CDCl_3$ solution in a ratio used in the synthesis reaction. Proton NMR was taken for this solution and solutions of individual precursors and are shown below. By comparing the mixture NMR spectrum with the NMR spectra of precursors, one can tell that the polyenal moiety of the donor-bridge compound forms complex with the pillar[5]arene as the vinylenic protons are no longer seen. In fact, those peaks are just broadened so much that are not observable unless the spectrum is blown up many times. This also indicates that the complex formed is dynamic as the proton NMR of CC14 clearly shows these vinylenic protons. It is also clear that the phenylene unit of D-B is not covered/encapsulated by the pillar[5]arene as the phenyl protons are neither broadened or shifted. Also, the acceptor proton signals are not changed in the proton NMR of the mixture, indicating that the acceptor is bulky enough not to fit into the pillar[5]arene cavity, which makes the acceptor a right choice as an end capper.

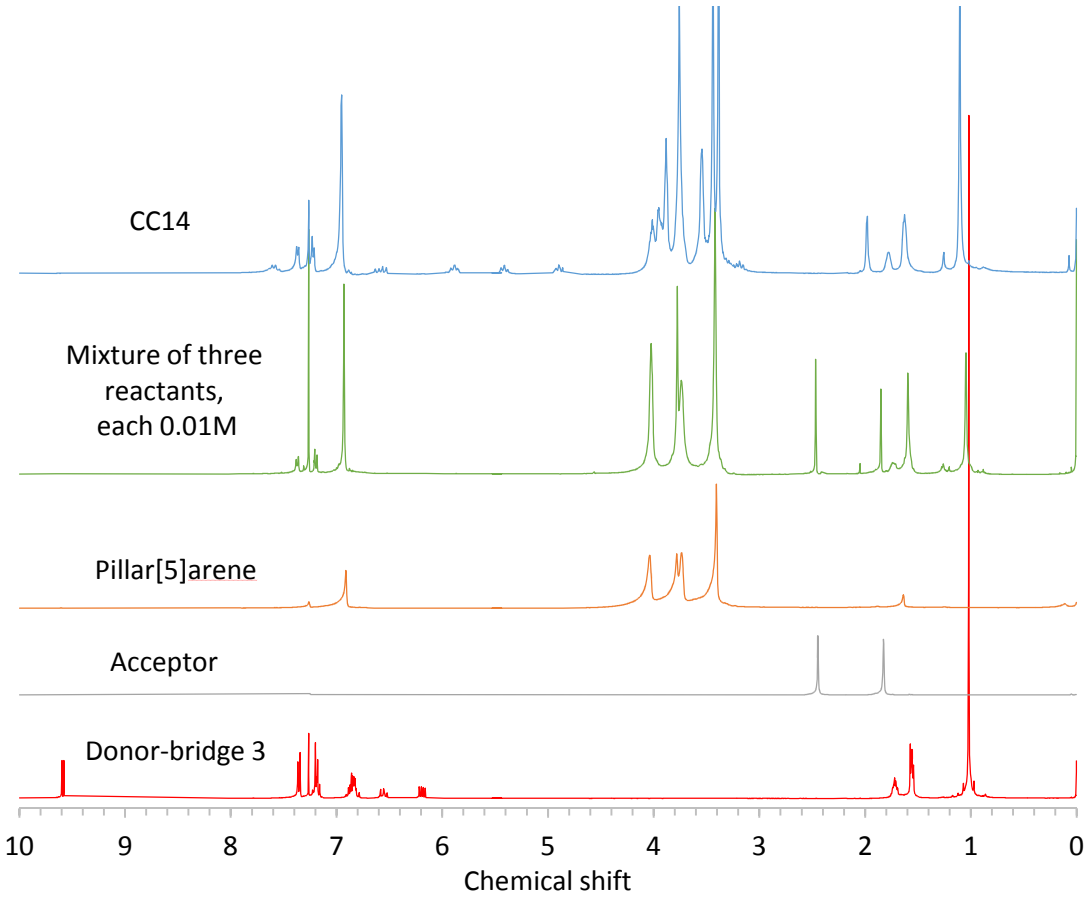

Figure 4.1: ^{1}H NMR of donor-bridge (DB3), acceptor (CF_3-TCF), and 1,4-bis(2-methoxyethoxy)pillar[5]ene, similar to CC14 but trienal peaks suppressed, presence of acceptor peaks and CH_2 peaks from donor TMP.

The large shift of conjugated protons in the spectrum of CC14 to the upper field is a clear evidence of the encapsulation of chromophore. In CC14 the donor 2,2,6,6-tetramethylpiperidine (TMP) subunit has CH_2 visible in the spectra meaning its signal was not affected by the pillar[5]arene. Very little shift is observed for the protons on the benzene of the chromophore, indicating that the pillar[5]arene mostly rest on the polyene moiety. CC14 has peak wavelengths at 666 nm (Figure 12), and shows blue color in its chloroform solution.

4.2 Photostability and Photodegradation Analysis

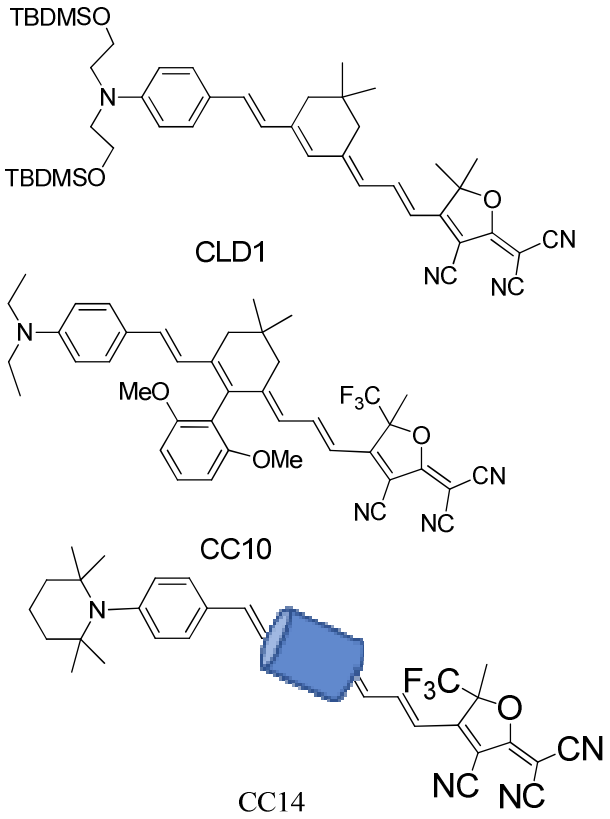

Figure 4.2: List of other notable chromophores and MLE chromophores.

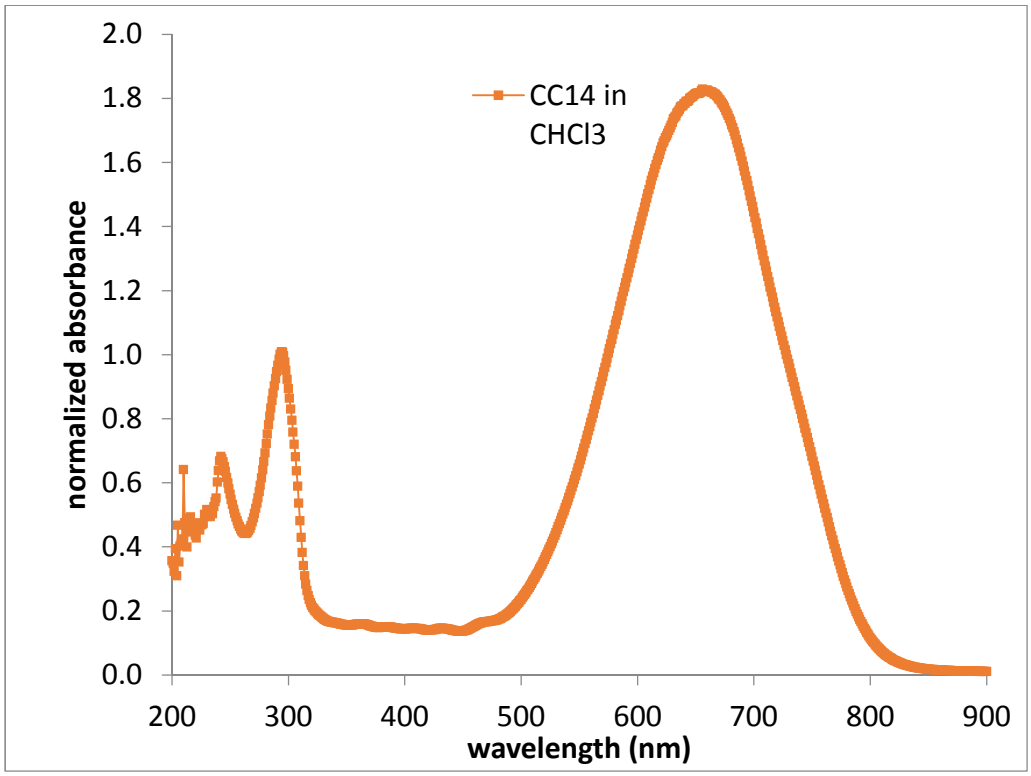

Figure 4.3: UV-vis absorbance spectra of CC14

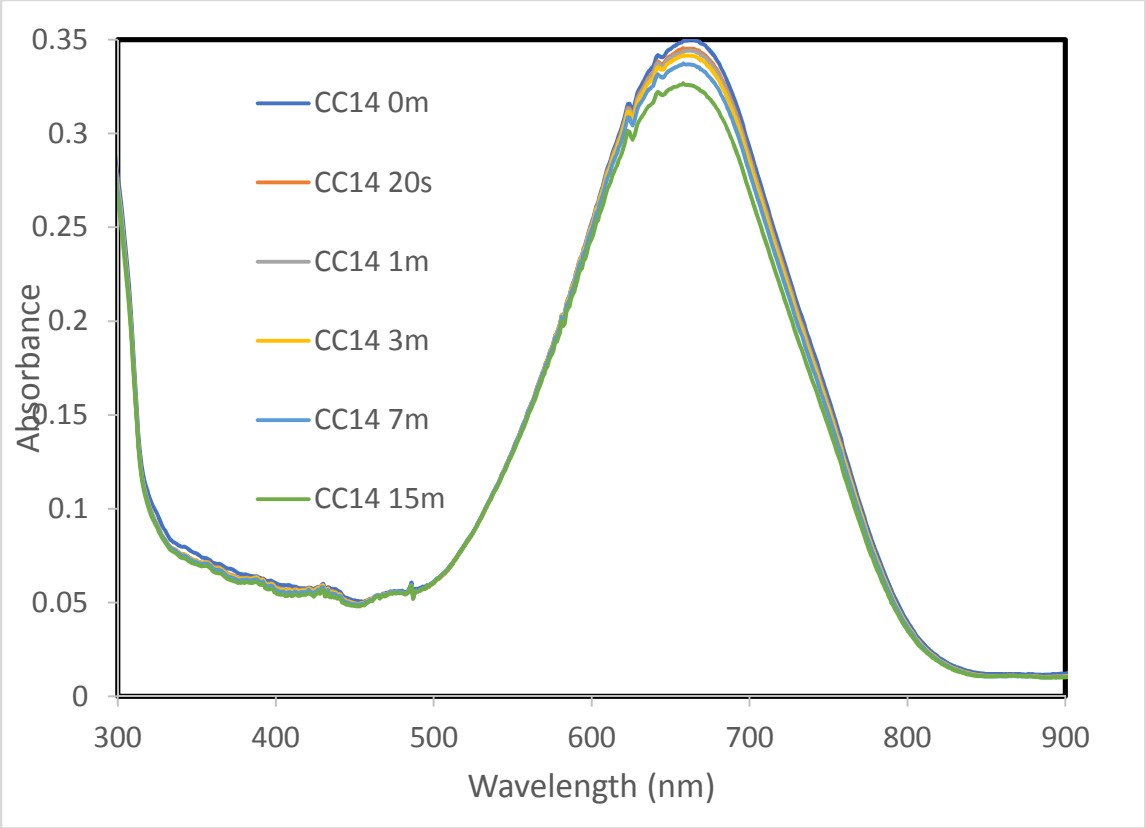

Figure 4.4: UV-vis absorption spectra of CC14 film with different time of illumination

Photostability of CC14 and other EO chromophores used for comparison was done using a xenon arc lamp. The lamp provides high intensity light that is 20-26 times that of the standard sun. Use of the strong light shortens photodegradation testing time.

The decay rate of the conjugated material can be expressed as

$$\frac{dC}{dt} = -kC \cdot I \cdot [O_2], \qquad (1)$$

where C is polymer concentration, I is the light intensity, and $[O_2]$ is oxygen concentration.

Since *I* and [O_2] are constant, and *C* is linearly related to *A* (peak absorbance), equation 1 can be rewritten as

$$\frac{dA}{dt} = -k'A \qquad (2)$$

Or the first order rate law for photodegradation is illustrated by equation 3

$$log\frac{A}{A_0} = -Kt, \qquad (3)$$

where K is the effective photodegradation constant, A_0 is the initial peak absorbance of film, and A/A_0 is the normalized peak absorbance.

UV-vis absorbance spectra of the CC14 (doped in an amorphous polycarbonate) film before illumination and after illumination of different amounts of time are shown in Figure 13. CC14 decomposed by 7% after 15 minutes. This is a very long time compared to other dyes like CLD1 that loses its color much earlier. Log A/A_0 is plotted as a function of time in Figure 14, where comparing different chromophores (CLD1, CC10) with the 1,4-bis(2-methoxyethoxy)pillar[5]arene protected chromophore (CC14). So, based on the slopes, CC14 is more stable than CC10 by about 11 times and 70 times more stable than CLD1. This research shows that once MLE occurs, the stability of the chromophore can be increased substantially. Other chromophores like CLD1 and CC10 will simply degrade because they are not protected by a bulky host molecule. Again, the stabilization is due to the encapsulation of the polyene backbone, which is more efficient than the bulky group (dimethoxyphenyl) used in CC10.

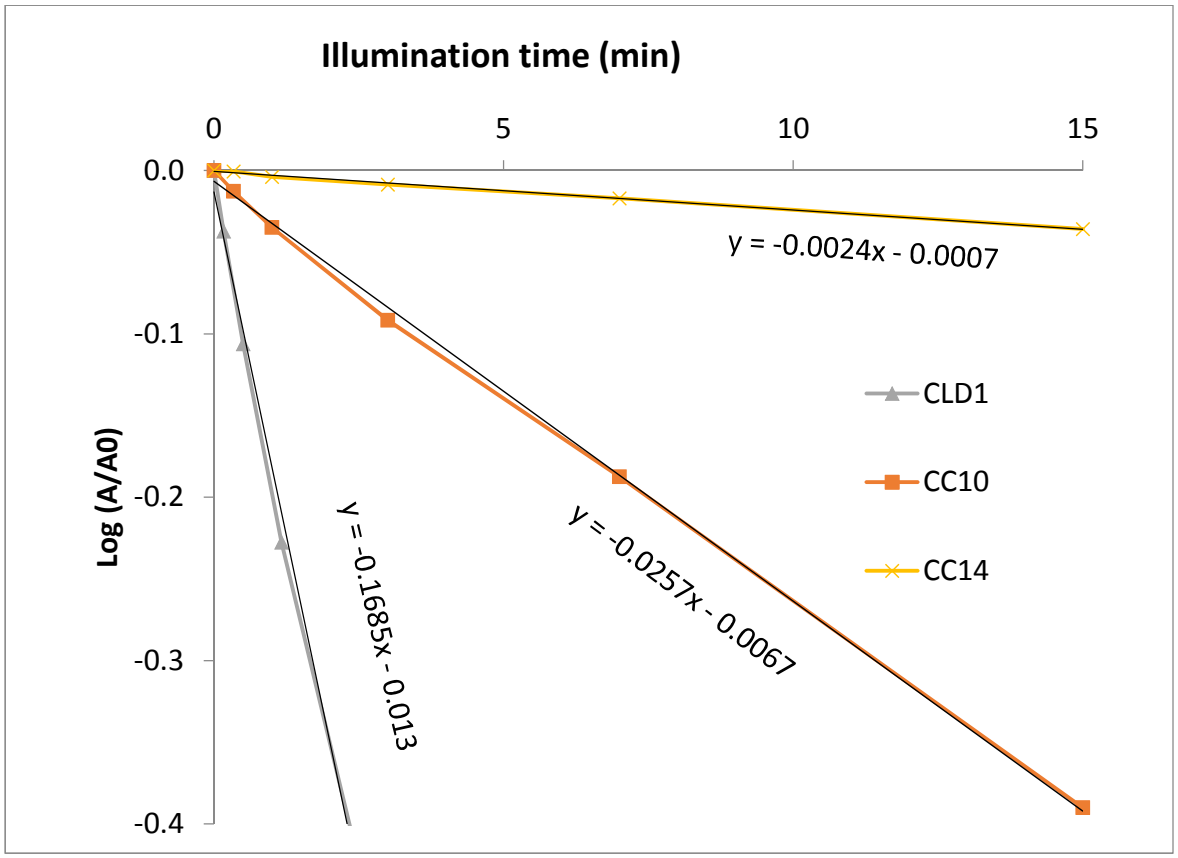

Figure 4.5: Semi-log plot of peak absorbance vs. illumination time of three different chromophores

4.3 Future Outlook on Photostability and Pillar[5]arenes

The goal of the research is to develop EO chromophores that allow the EO devices to operate in the air during the whole lifetime (10 years or longer). An enhancement of five order of magnitude in photostability is needed to reach the goal. The following strategies will be explored to further enhance photostability of EO chromophores:

1. More complete protection of the bridge.

In CC14, the rigid portion of the pillar[5]arene ring is not long enough to protect all four C=C bonds in the bridge. The research in ongoing to put two rings on the donor-bridge.

2. Develop and employ new electron acceptors that do not have C=C bonds

In CC14, the acceptor has two C=C bonds that are still susceptible to reaction with singlet oxygen and radical oxygen anion. Development of new electron acceptor provides additional potential for photostability enhancement.

3. Study photodegradation mechanisms of encapsulated chromophores to identifying remaining mechanisms of photodegradation.

The photodecomposition mechanism can also be studied using cyclic voltammetry (CV), FT-IR, HPLC and GPC. Such study has conducted by the group earlier on some polymers. These careful analyses can determine the nature of reactive oxygen species involved in photodegradation, which can help deduce the degradation pathway involved. By using CV, we can help elucidate the photodegradation process by determining the LUMO and HOMO levels significance to degradation. So, the effect of O_2 anion mechanism, that requires electron transfer from an excited organic material to diatomic oxygen can be observed. This can help determine if radical superoxide anions (O_2^-) are responsible for photodegradation. Similarly, in some IR spectra radical superoxide anions (O_2^-) can be determined responsible if the C-H stretching peaks will decrease with time or adding radical scavengers (ex. BHT). Also, while using FT-IR, if the integration of C-H stretching peak in IR spectra does not change with illumination time, the degradation mechanism could be that of the singlet oxygen mechanism because singlet oxygen does

not react with alkyl groups. NMR, GPC and HRMS can be used to identify photodegradation products, changes in molecular weight, and thus help establish decomposition pathways and identify the weaknesses of MEC structures, whether it is the donor bridge, acceptor or host pillar[5]arene. Studying the mechanism of the degradation will lead to the generation of new ideas for further enhancement of photostability and understanding of how encapsulation plays a role in photochemical stability.

4. The development of methods to improve yield are a paramount concern.

Often, yields for MECs were abysmally low, sometimes not enough for NMR and calling for many repetitions in synthesis. So, changing from conventional and traditional synthetic techniques need to be explored, since steric factors of the host pillar[5]arene structure and the bulky capped ends may be responsible for low yields. To improve yield, the reactants must be miscible in each other, because many reactions involving large host molecules and shorter guest chromophores (see figure 3.1) did not work. Additionally, different solvents or a combination of solvent need to be used to carry out the reactions. Solvent-free reactions may not work because the melting points of reactants are different than the optimal temperature for the reaction to proceed. So, adding compounds that reduce melting points could be an option. Another way to make solvent free reactions work is by making solutions of reactants, mixing them then removing solvent. But this may lead to crystals forming. Last method is to place the reaction in a sealed reactor under high pressure with a nitrogen environment since this can force bulky molecules to interact with each other. Removing air from the reactor could also be done to reduce oxygen from affecting the reactants and MECs products.

4.4 Summary and Conclusion

This study aims to synthesize a new type of EO material via MLE. Photostability is an important when improving on these new materials. The photostability of the new materials is an essential parameter that needs to be tested. The donor-bridge, acceptor and pillar[n]arene structure were chosen as novel reactants in the encapsulation procedure. There remain other factors that need to be tested in this method: morphological changes, degradation mechanisms and computational studies.

In closing, we developed a new strategy to encapsulate electrooptic chromophores with pillar[n]arene host molecules. Synthesized donor-bridge and pillar[n]arenes with side groups. Based on NMR, discovered pillar[n]arene does rest on trienal moiety and both donor and acceptor are good at capping either end. Also, encapsulation likely does not affect absorbance of π- conjugated backbone. But, the photostability of CC14 is greater than the other chromophores CC10 and CLD1. Showing that the overall photostability does increase based on encapsulation, as the pillar[n]arene structure is a ‘sacrificial’ group that prevents rapid photodegradation.

REFERENCES

1) Xu, T.; Yu, L., How to design low bandgap polymers for highly efficient organic solar cells. *Materials Today* **2014,** *17* (1), 11-15.

2) Dalton, L. R.; Sullivan, P. A.; Bale, D. H., Electric Field Poled Organic Electro-optic Materials: State of the Art and Future Prospects. *Chem. Rev.* **2009,** *110*, 25.

3) Dalton, L. R.; Benight, S. J.; Johnson, L. E.; Daniel B Knorr, J.; Kosilkin, I.; Eichinger, B. E.; Robinson, B. H.; Jen, A. K.-Y.; Overney, R. M., Systematic Nanoengineering of Soft Matter Organic Electro-optic Materials. *Chem. Mater* **2011,** *23*, 430–445

4) Duran-Sampedro, G.; Agarrabeitia, A. R.; Garcia-Moreno, I.; Costela, A.; Banuelos, J.; Arbeloa, T.; Arbeloa, I. L.; Chiara, J. L.; Ortiz, M. J., Chlorinated BODIPYs: Surprisingly Efficient and Highly Photostable Laser Dyes. *Eur. J. Org. Chem.* **2012,** *2012* (32), 6335–6350.

5) Navarro-Fuster, V.; Calzado, E. M.; Boj, P. G.; Quintana, J. A.; Villalvilla, J. M.; Diaz-Garcia, M. A.; Trabadelo, V.; Juarros, A.; Retolaza, A.; Merino, S., Highly photostable organic distributed feedback laser emitting at 573 nm. *Appl. Phys. Lett.* **2010,** *97*, 171104.

6) Perepichka, D. F.; Perepichka, I. F.; Meng, F.; Wudl, F., Light-emitting polymers. *Opt. Sci. Eng.* **2007,** *111*, 45-293.

7) Wu, H.; Ying, L.; Yang, W.; Cao, Y., Progress and perspective of polymer white light-emitting devices and materials. *Chem. Soc. Rev.* **2009,** *38* (12), 3391-3400.

8) Salhi, A.; S., M.; Alam, J.; Dass, L. A.; Raja, M., Recent advances in conjugated polymers for light emitting devices. *Int. J. Mol. Sci.* **2011,** *12*, 2036-2054.

9) Kaeser, A.; Schenning, A. P. H. J., Fluorescent Nanoparticles Based on Self□Assembled π□Conjugated Systems. *Adv. Mater.* **2010,** *22*, 2985–2997.

10) Li, K.; Liu, B., Water-soluble conjugated polymers as the platform for protein sensors. *Polym. Chem.* **2010,** *1* (3), 252-259.

11) Li, K.; Liu, B., Polymer encapsulated conjugated polymer nanoparticles for fluorescence bioimaging. *J. Mater. Chem.* **2012,** *22* (4), 1257-1264.

12) Feng, X.; Liu, L.; Wang, S.; Zhu, D., Water-soluble fluorescent conjugated polymers and their interactions with biomacromolecules for sensitive biosensors. *Chem. Soc. Rev.* **2010,** *39* (7), 2411-2419.

13) Alvarez, A.; Costa-Fernandez, J. M.; Pereiro, R.; Sanz-Medel, A.; Salinas-Castillo, A., Fluorescent conjugated polymers for chemical and biochemical sensing. *Trends Anal. Chem.* **2011,** *30* (8), 1513–1525.

14) Kim, H. N.; Ren, W. X.; Kim, J. S.; Yoon, J., Fluorescent and colorimetric sensors for detection of lead, cadmium, and mercury ions. *Chem. Soc. Rev.* **2012,** *41* (8), 3210-3244.

15) Kim, H. N.; Guo, Z.; Zhu, W.; Yoon, J.; Tian, H., Recent progress on polymer-based fluorescent and colorimetric chemosensors. *Chem. Soc. Rev.* **2011,** *40*, 79-93.

16) Hu, J.; Liu, S., Responsive polymers for detection and sensing applications: current status and future developments. *Macromolecules* **2010,** *43*, 8315–8330.

17) Yui, T.; Tamaki, Y.; Sekizawa, K.; Ishitani, O., Photocatalytic reduction of CO_2: from molecules to semiconductors. *Top. Curr. Chem.* **2011,** *303*, 151–184.

18) Grills, D. C.; E. Fujita, 2010, 1, , New Directions for the Photocatalytic Reduction of CO_2: Supramolecular, $scCO_2$ or Biphasic Ionic Liquid− $scCO_2$ Systems. *J. Phys. Chem. Lett.* **2010,** *1*, 2709–2718.

19) Esswein, A. J.; Nocera, D. G., Hydrogen production by molecular photocatalysis. *Chem. Rev.* **2007,** *107*, 4022–4047.

20) Williams, G. V. M.; Kutuvantavida, Y.; Janssens, S.; Raymond, S. G.; Do, M. T. T.; Bhuiyan, M. D. H.; Quilty, J. W.; Denton, N.; Kay, A. J., The effects of excited state lifetime, optical intensity, and excited state quenchers on the photostability of zwitterionic chromophores. *J. Appl. Phys.* **2011,** *110*, 083524.

21) Zhang, C.; Dalton, L. R.; Oh, M.-C.; Zhang, H.; Steier, W. H., Low Vpi EO Modulators from CLD-1: Chromophore Design and Synthesis, Material Processing and Characterization. *Chem. Mater.* **2001,** *13* (9), 3043-3050.

22) Cigáň, M.; Gáplovský, A.; Sigmundová, I.; Zahradník, P.; Dědic, R.; Hromadová, M., Photostability of D–p–A nonlinear optical chromophores containing a benzothiazolium Acceptor. *J. Phys. Org. Chem.* **2011,** *24*, 450–459.

23) Tada, K.; Onoda, M., Photoinduced modification of photoluminescent and electroluminescent properties in poly(p-phenylene vinylene) derivative. *J. App. Phys.* **1999,** *86*, 3134.

24) Tromholt, T.; Madsen, M. V.; Carlé, J. E.; Helgesen, M.; Krebs, F. C., Photochemical stability of conjugated polymers, electron acceptors and blends for polymer solar cells resolved in terms of film thickness and absorbance. *J. Mater. Chem.* **2012,** *22*, 7592-7601.

25) Manceau, M.; Bundgaard, E.; Carlé, J. E.; Hagemann, O.; Helgesen, M.; Søndergaard, R.; Jørgensen, M.; Krebs, F. C., Photochemical stability of □-conjugated polymers for polymer solar cells: a rule of thumb. *J. Mater. Chem.* **2011,** *21*, 4132-4141.

26) Cao, H.; Weidong, H.; Mao, Y.; Lin, X.; Ishikawa, K.; Dickerson, J. H.; Hess, W. P., Recent progress in degradation and stabilization of organic solar cells. *J. Power Sources* **2014,** *264*, 168-183.

27) Gouterman, M. The Porphyrins 1978, 1–165

28) Scheer, H. Advances in Photosynthesis and Respiration Chlorophylls and Bacteriochlorophylls 2006, 1–26.

29) Stanoeva, T.; Neshchadin, D.; Gescheidt, G.; Ludvik, J.; Lajoie, B.; Batchelor, S. N. The Journal of Physical Chemistry A 2005, 109 (49), 11103–11109.

30) Sanow, L. P.; Sun, J.; Zhang, C., Photostability of Two Dicyano-Substituted Poly(phenylenevinylenes) with Different Side Chains. *J. Poly. Sci. A* **2015**, DOI: 10.1002/pola.27755.

31) Chambon, S.; Rivaton, A.; Gardette, J.-L.; Firon, M., Reactive intermediates in the initiation step of the photo□oxidation of MDMO□PPV. *J. Polym. Sci., Part A: Polym. Chem.* **2009,** *47*, 6044–6052.

32) Chambon, S.; Rivaton, A.; Gardette, J. L.; Firon, L., Photo- and thermo-oxidation of poly(p-phenylene-vinylene) and phenylene-vinylene oligomer. *Polym. Degrad. Stab.* **2011,** *96*, 1149-1158.

33) Hoke, E. T.; Sachs-Quintana, I. T.; Lloyd, M. T.; Kauvar, I.; Mateker, W. R.; Nardes, A. M.; Peters, C. H.; Kopidakis, N.; McGehee, M. D., The role of electron affinity in determining whether fullerenes catalyze or inhibit photooxidation of polymers for solar cells. *Adv. Energy Mater.* **2012,** *2*, 1351-135.

34) Chambon, S.; Rivaton, A.; Gardette, J. L.; Firon, M.; Lutsen, L., Aging of a Donor Conjugated Polymer: Photochemical Studies of the Degradation of Poly[2-methoxy-5-(3',7'-dimethyloctyloxy)-1,4-phenylenevinylene]. *J. Polym. Sci., Part A: Polym. Chem.* **2007,** *45*, 317-331.

35) Manceau, M.; Rivaton, A.; Gardette, J. L.; Guillerez, S.; Lemaitre, N., The mechanism of photo- and thermooxidation of poly(3-hexylthiophene) (P3HT) reconsidered. *Polym. Degrad. Stab.* **2009,** *94*, 898-907.

36) Dam, N.; Scurlock, D.; Wang, B.; Ma, L.; Sundahl, M.; Ogilby, P. R., Singlet oxygen as a reactive intermediate in the photodegradation of phenylenevinylene oligomers. *Chem. Mater.* **1999,** *11*, 1302-1305.

37) Vulic, I.; Vitarelli, G.; Zenner, J. M., Structure–property relationships: phenolic antioxidants with high efficiency and low colour contribution. *Polym. Degrad. Stab.* **2002,** *78* (1), 27–34.

38) Ogryzlo, E. A.; Tang, C. W., Quenching of Oxygen (singlet state) by amines. *J. Am. Chem. Soc.* **1970,** *92* (17), 5034-5036.

39) Moura, J. C. V. P.; Oliveira-Campos, A. M. F.; Griffiths, J., The effect of additives on the photostability of dyed polymers. *Dyes and Pigments* **1997,** *33*, 173–196.

40) Halliwell, B.; Murcia, M. A.; Chirico, S.; Aruoma, O. I., Free radicals and antioxidants in food and in vivo: What they do and how they work. *Critical Reviews in Food Science and Nutrition* **1995,** *35* (1-2), 7-20.

41) Sun, J.; Sanow, L. P.; Sun, S. S.; Zhang, C., Dicyano-Substituted Poly (phenylenevinylene)(DiCN–PPV) and the Effect of Cyano Substitution on Photochemical Stability. *Macromolecules* **2013,** *46*, 4247-4254.

42) Alem, S.; Wakim, S.; Lu, J.; Robertson, G.; Ding, J.; Tao, Y., Degradation Mechanism of Benzodithiophene-Based Conjugated Polymers when Exposed to Light in Air. *ACS Appl. Mater. Interfaces* **2012,** *4*, 2993–2998.

43) Sun, H.; Putta, A.; Kloster, J. P.; Tottempudi, U. K., Unexpected photostability improvement of aromatics in polyfluorinated solvents. *Chem. Commun.* **2012,** *48*, 12085-12087.

44) Soon, Y. W.; Cho, H.; Low, J.; Bronstein, H.; McCulloch, I.; Durrant, J. R., Correlating triplet yield, singlet oxygen generation and photochemical stability in polymer/fullerene blend films. *Chem. Commun.* **2013,** *49*, 1291-1293.

45) Teyssandier, J.; Feyter, S. D.; Mali, K. S. Chemical Communications 2016, 52 (77), 11465–11487.

46) Forbes, C. C.; Smith, B. D., Improving the Properties of Organic Dyes by Molecular Encapsulation, Easwaran Arunkumar. *Eur. J. Org. Chem.* **2005,** *2005* (19), 4051–4059.

47) Bruns, C. J.; Stoddart, J. F., Rotaxane-Based Molecular Muscles. *Acc. Chem. Res.* **2014,** *47*, 2186−2199.

48) Xue, M.; Yang, Y.; Chi, X.; Ya, X.; Feihe Huang, 2015, Development of Pseudorotaxanes and Rotaxanes: From Synthesis to Stimuli-Responsive Motions to Applications. *Chem. Rev.* **2015,** *115* (15), 7398–7501.

49) Mandal, A. K.; Gangopadhyay, M.; Das, A., Photo-responsive pseudorotaxanes and assemblies,. *Chem. Soc. Rev.* **2015,** *44* (3), 663-676.

50) Leigh, D. A.; Marcos, V.; Wilson, M. R., Rotaxane Catalysts. *ACS Catalysis* **2014,** *4* (12), 4490-4497.

51) Niess, F.; Duplan, V.; Sauvage, J.-P., Molecular muscles: from species in solution to materials and devices. *Chem. Lett.* **2014,** *43* (7), 964-974.

52) Kolmar, H. Alternative binding proteins: Biological activity and therapeutic potential of cystine-knot miniproteins. FEBS Journal. **2008**, 275 (11), 2684–2690.

53) Yamagishi, Y.; Kaino, T.; Kameyama, A.; Nishikubo, T. Polymers of photoreactive calixarene derivatives for optical applications. Organic Photonic Materials and Devices V. **2003**.

54) Buschmann, H.-J.; Cleve, E.; Mutihac, L.; Schollmeyer, E. A novel experimental method for the study of complex formation between α-, β- and γ-cyclodextrin and nearly insoluble cucurbituril– [2]rotaxanes in aqueous solution. *Microchemical Journal*. **2000**, 64 (1), 99–103.

55) Wheate, N. J.; Limantoro, C. Cucurbit[n]urils as excipients in pharmaceutical dosage forms. *Supramolecular Chemistry*. **2016**, 28 (9-10), 849–856.

56) Zhang, H.; Liu, L.; Gao, C.; Sun, R.; Wang, Q. Enhancing photostability of cyanine dye by cucurbituril encapsulation. Dyes and Pigments. **2012**, 94 (2), 266–270.

57) Kaliappan, R.; Maddipatla, M. V. S. N.; Kaanumalle, L. S.; Ramamurthy, V. Crystal engineering principles applied to solution photochemistry: controlling the photodimerization of stilbazolium salts within γ-cyclodextrin and cucurbit[8]uril in water. *Photochem. Photobiol. Sci*. **2007**, 6 (7), 737–740.

58) Guether, R.; Reddington, M. V., Photostable cyanine dye β-cyclodextrin conjugates. *Tetrahedron Lett.* **1997,** *38*, 6167-6170.

59) Buston, J. E. H.; Young, J. R.; Anderson, H. L., Rotaxane-encapsulated cyanine dyes: enhanced fluorescence efficiency and photostability. *Chem. Commun.* **2000**, 905–906.

60) Ogoshi, T.; Yamagishi, T.-a., Pillararenes: Versatile Synthetic Receptors for Supramolecular Chemistry. *Eur. J. Org. Chem.* **2013**, 2961–2975.

61) Ogoshi, T.; Kayama, H.; Aoki, T.; Yamagishi, T.-a.; Ohashi, R.; Mizuno, M., Extension of polyethylene chains by formation of polypseudorotaxane structures with perpentylated pillar[5]arenes. *Polym. J.* **2014,** *46*, 77–81.

62) Ogoshi, T.; Aoki, T.; Ueda, S.; Tamura, Y.; Yamagishi, T.-a., Pillar[5]arene-based nonionic polyrotaxanes and a topological gel prepared from cyclic host liquids. *Chem. Commun.* **2014,** *50*, 6607-6609.

63) Kitajima, K.; Ogoshi, T.; Yamagishi, T.-a., Diastereoselective synthesis of a [2]catenane from a pillar[5]arene and a pyridinium derivative. *Chem. Commun.* **2014,** *50*, 2925-2927.

64) Aoki, T.; Ogoshi, T.; Yamagishi, T.-a., Chemically Responsive Supramolecular Structural Change of Pillar[5]arene Nanotubes. *Chem. Lett.* **2011,** *40*, 795-797.

65) Ogoshi, T.; Nishida, Y.; Yamagishi, T.-a.; Nakamoto, Y., High Yield Synthesis of Polyrotaxane Constructed from Pillar[5]arene and Viologen Polymer and Stabilization of Its Radical Cation. *Macromolecules* **2010,** *43*, 7068–7072.

66) Ogoshi, T.; Nishida, Y.; Yamagishi, T.-a.; Nakamoto, Y., Polypseudorotaxane Constructed from Pillar[5]arene and Viologen Polymer. *Macromolecules* **2010,** *43*, 3145–3147.

67) Ogoshi, T.; Kanai, S.; Fujinami, S.; Yamagishi, T.; Nakamoto, Y., *para*-Bridged Symmetrical Pillar[5]arenes: Their Lewis Acid Catalyzed Synthesis and Host–Guest Property. *J. Am. Chem. Soc.* **2008,** *130*, 5022–5023.

68) Holler, M.; Allenbach, N.; Sonet, J.; Nierengarten, J.-F. The high yielding synthesis of pillar[5]arenes under Friedel-Crafts conditions explained by dynamic covalent bond formation. Chem. Commun. 2012, 48, 2576.

69) Ogoshi, T.; Ueshima, N.; Akutsu, T.; Yamafuji, D.; Furuta, T.; Sakakibara, F.; Yamagishi, T.-A. The template effect of solvents on high yield synthesis, co-cyclization

of pillar[6]arenes and interconversion between pillar[5]- and pillar[6]arenes Chem. Commun. **2014**, 50 (43), 5774–5777.

70) Ogoshi, T.; Ueshima, N.; Sakakibara, F.; Yamagishi, T.-A.; Haino, T. Conversion from Pillar[5]arene to Pillar[6–15]arenes by Ring Expansion and Encapsulation of C60 by Pillar[n]arenes with Nanosize Cavities. *Organic Letters.* **2014**, 16(11), 2896–2899.

71) Wheate, N. J.; Dickson, K.-A.; Kim, R. R.; Nematollahi, A.; Macquart, R. B.; Kayser, V.; Yu, G.; Church, W. B.; Marsh, D. J. Host-Guest Complexes of Carboxylated Pillar[n]arenes With Drugs. *Journal of Pharmaceutical Sciences*. **2016**, 105 (12), 3615–3625.

72) Song, N.; Chen, D.-X.; Qiu, Y.-C.; Yang, X.-Y.; Xu, B.; Tian, W.; Yang, Y.-W. Stimuli-Responsive Blue Fluorescent Supramolecular Polymers Based on a Pillar[5]arene Tetramer. *Chem. Commun*. **2014**, 50, 8231–8234.

73) Moretti, E.; Talon, A.; Storaro, L.; Donne, A. L.; Binetti, S.; Benedetti, A.; Polizzi, S., Concentration quenching and photostability in Eu(dbm)3phen embedded in mesoporous silica nanoparticles. *J. Lumin.* **2014,** *146*, 178–185.

74) Wu, X.; Zhu, W., Stability enhancement of fluorophores for lighting up practical application in bioimaging. *Chem. Soc. Rev.* **2015,** *44* (13), 4179-4184.

75) Walenzyk, T.; Carola, C.; Buchholz, H.; Koenig, B., Synthesis of mono-dispersed spherical silica particles containing covalently bonded chromophores. *Inter. J. Cosmetic Sci.* **2005,** *27* (3), 177-189.

76) Alonso, R.; Yamaji, M.; Jiménez, M. C.; Miranda, M. A., Enhanced Photostability of the Anthracene Chromophore in Aqueous Medium upon Protein Encapsulation. *J. Phys. Chem. B* **2010,** *114*, 11363–11369.

77) Aeunkumar, E.; Fu, N.; Smith, B. D., Squaraine-derived rotaxanes: highly fluorescent Near-IR dyes. *Chem. Eur. J.* **2006,** *12*, 4684 – 4690.

78) Anderson, S.; Claridge, T. D. W.; Anderson, H. L., Azo□dye rotaxanes. *Angew. Chem. Int. Ed. Engl.* **1997,** *36*, 1310–1313.

79) Haque, S. A.; Park, J. S.; Srinivasarao, M.; Durrant, J. R., Molecular-level insulation: an approach to controlling interfacial charge transfer. *Adv. Mater.* **2004,** *16*, 1177-1181.

80) Shi, Y.; Wang, W.; Lin, W.; Olson, D. J.; Bechtel, J. H., Double-end crosslinked electro-optic polymer modulators with high optical power handling capability. *Appl. Phys. Lett.* **1997,** *70* (11), 1342-1344.

81) Foucher, C.; Guilhabert, B.; Herrnsdorf, J.; Laurand, N.; Dawson, M. D., Diode-pumped, mechanically-flexible polymer DFB laser encapsulated by glass membranes. *Optics Express* **2014,** *22* (20), 24160-24168.

82) Monguzzi, A.; Frigoli, M.; Larpent, C.; Meinardi, F., Laser dye doped nanoparticles for highly photostable optical nanoamplifiers. *RSC Advances* **2012,** *2*, 11731–11736.

83) Liu, J.; GuangmingXu; FenggangLiu; Kityk, I.; XinhouLiu; ZhenZhen, Recent advancesinpolymerelectro-optic modulators. *RSC Adv.* **2015,** *5*, 15784-15794.

84) Levi, L.; Mueller, T. J. J. Multicomponent Syntheses of Functional Chromophores. ChemInform 2016, 47 (29).

85) Dalton, L. R. Organic electro-optics and photonics: molecules, polymers and crystals; Cambridge University Press: Cambridge, 2015.

86) Luo, J.; Jen, A. K.-Y., Highly Efficient Organic Electrooptic Materials and Their Hybrid Systems for Advanced Photonic Devices. *IEEE J. Sel. Top. Quantum Electron.* **2013,** *19* (6), 3401012.

87) Johnson, L. E.; Dalton, L. R.; Robinson, B. H., Optimizing Calculations of Electronic Excitations and Relative Hyperpolarizabilities of Electrooptic Chromophores. *Acc. Chem. Res.* **2014,** *47*, 3258−3265.

88) Kim, T.-D.; Lee, K.-S., D-π-A Conjugated Molecules for Optoelectronic Applications. *Macromol. Rapid Commun.* **2015,** *36*, 943−958.

89) Pickett, J. E. Review and kinetic analysis of the photodegradation of UV absorbers. *Macromolecular Symposia*. **1997**, 115 (1), 127–141.

90) Yousif, E.; Haddad, R. Photodegradation and photostabilization of polymers, especially polystyrene: review. *SpringerPlus*. **2013**, 2 (1), 398.

91) IARC Working Group on the Evaluation of Carcinogenic Risk to Humans. GENERAL INTRODUCTION TO THE CHEMISTRY OF DYES https://www.ncbi.nlm.nih.gov/books/NBK385442/ (accessed 2017).